Am J Blood Res 2015;5(2):34-61
www.AJBlood.us /ISSN:2160-1992/AJBR0020858

Original Article

A novel interaction between megakaryocytes and activated fibrocytes increases TGF-β bioavailability in the *Gata1^{low}* mouse model of myelofibrosis

Maria Zingariello[1*], Alessandra Ruggeri[2*], Fabrizio Martelli[3], Manuela Marra[3], Laura Sancillo[4], Ilaria Ceglia[5], Rosa Alba Rana[4], Anna Rita Migliaccio[2,5]

[1]Unit of Microscopic and Ultrastructural Anatomy, Department of Medicine, Campus Bio-Medico University Rome, Italy; [2]Biomedical and Neuromotory Sciences, Alma Mater University, Bologna, Italy; [3]Hematology, Oncology and Molecular Medicine and Department of Cell Biology and Neuroscience, Istituto Superiore di Sanità, Rome, Italy; [4]Medicine and Aging Science, University G. D'Annunzio of Chieti-Pescara, Italy; [5]Tisch Cancer Institute, Ichan School of Medicine at Mount Sinai, New York, NY, USA. [*]Equal contributors.

Received November 30, 2015; Accepted December 15, 2015; Epub December 25, 2015; Published December 30, 2015

Abstract: Despite numerous circumstantial evidences, the pathogenic role of TGF-β in primary myelofibrosis (PMF), the most severe of the Philadelphia-negative myeloproliferative neoplasms, is still unclear because of the modest (2-fold) increases in its plasma levels observed in PMF patients and in the *Gata1^{low}* mouse model. Whether myelofibrosis is associated with increased bioavailability of TGF-β bound to fibrotic fibres is unknown. Transmission electron-microscopy (TEM) observations identified that spleen from PMF patients and *Gata1^{low}* mice contained megakaryocytes with abnormally high levels of TGF-β and collagen fibres embedded in their cytoplasm. Additional immuno-TEM observations of spleen from *Gata1^{low}* mice revealed the presence of numerous activated fibrocytes establishing with their protrusions a novel cellular interaction, defined as peripolesis, with megakaryocytes. These protrusions infiltrated the megakaryocyte cytoplasm releasing collagen that was eventually detected in its mature polymerized form. Megakaryocytes, engulfed with mature collagen fibres, acquired the morphology of para-apoptotic cells and, in the most advanced cases, were recognized as polylobated heterochromatic nuclei surrounded by collagen fibres strictly associated with TGF-β. These areas contained concentrations of TGF-β-gold particles ~1000-fold greater than normal and numerous myofibroblasts, an indication that TGF-β was bioactive. Loss-of-function studies indicated that peripolesis between megakaryocytes and fibrocytes required both TGF-β, possibly for inducing fibrocyte activation, and P-selectin, possibly for mediating interaction between the two cell types. Loss-of-function of TGF-β and P-selectin also prevented fibrosis. These observations identify that myelofibrosis is associated with pathological increases of TGF-β bioavailability and suggest a novel megakaryocyte-mediated mechanism that may increase TGF-β bioavailability in chronic inflammation.

Keywords: Megakaryocytes, activated fibrocytes, neutrophils, TGF-β, P-selectin, myelofibrosis

Introduction

Patients with primary myelofibrosis (PMF), the most severe of the Philadelphia-negative myeloproliferative neoplasms, experience progressive fibrosis eventually leading to hematopoietic failure in the bone marrow and develop extramedullary hematopoiesis in the spleen [1, 2]. Although the disease is associated with multiple primary lesions (65% with *JAK2*V617F mutation, 20% with CALR mutations and 15% with mutations in genes still to be identified) [3, 4], it is characterized by unique ultrastructural abnormalities in megakaryocyte development discovered for the first time in 1975 by Dr. Zucker-Franckin [5]. These ultrastructural abnormalities, which are suggestive of delayed maturation, were further characterized by other groups showing increased content of TGF-β in the cytoplasm [6] and P-selectin on the demarcation membrane system (DMS) [7] and reduced post-translation expression of GATA1, the transcription factor that control megakaryocytic maturation in the nucleus [8]. In addition, likely through increased P-selectin expression [9, 10], myelofibrotic megakaryocytes engage

in pathological emperipolesis with neutrophils leading to their death by an immuno-mediated process defined para-apoptosis [11, 12]. It has been suggested that pathological emperipolesis is directly responsible for fibrosis by favoring release of TGF-β activated by neutrophil proteases from the megakaryocyte cytoplasm into the extracellular space [13]. Circumstantial evidence that this interaction is responsible for triggering fibrosis is provided by the fact that, in addition to PMF patients, it is observed also in animal models, such as thrombopoietin high (TPO^{high}) [7] and *Gata1^{low}* [13] mice but is barely detectable when these animal models are treated by loss-of-function of TGF-β [14, 15]. Neutrophil emperipolesis with megakaryocytes has also been observed in other inflammatory pathologies (i.e. recovery after sub-lethal irradiation [16], aging [17] and altered megakaryocyte maturation induced by the gunmetal mutation [18]) associated with fibrosis. In spite of this overwhelming evidence, the observation that the levels of bioactive TGF-β in the plasma and marrow/spleen washes from PMF patients are only modestly greater (by 2-fold) than normal [15, 19] suggested that additional inflammatory cytokines may play a role more prominent than TGF-β in inducing fibrosis [20, 21].

TGF-β is a member of a large family of growth factors involved in tissue development and repair as well as in cancer progression [22, 23, 24]. TGF-β activity is mainly regulated at the protein level: it is released as a latent complex which is activated by proteolytic cleavage of the inhibitory domain of the protein [22] and stored in the microenvironment cross-linked to the extracellular matrix [25]. This storage, also known as bioavailability, plays an important role in the control of morphogenesis [25, 26]. Cross-linking of TGF-β to the extracellular matrix is an active process catalyzed by the latent TGF-β binding protein (LTBP) [27]. The best characterized of the LTBP substrates is fibrillin-1, a protein defective in the congenic bone growth retardations observed in Marfan Syndrome. Cross-linking of TGF-β to fibrillin-1 assures that the microenvironmental bio-availability of this growth factor reaches the levels necessary to activate the osteogenic potential of mesenchymal stem cells and to sustain bone formation [28]. Whether TGF-β may be also cross-linked to additional components of the extracellular matrix is unknown.

Our laboratory has characterized the ultrastructural abnormalities of megakaryocyte development occurring in the *Gata1^{low}* model of the disease for many years. The hypomorphic *Gata1^{low}* mutation deletes the first 5' enhancer of the gene, the hypersensitive site 1, that controls its expression in megakaryocytes [29]. In the C57BL6 background the mutation is embryonically lethal due to severe thrombocytopenia and anemia [30]. By contrast, in the CD1 background, *Gata1^{low}* mice are not anemic and have a normal life-span because they are capable to activate extramedullary hematopoiesis in spleen [31]. The mice, however, remain thrombocytopenic with megakaryocytes expressing reduced levels of *Gata1* mRNA. These reductions are comparable to those observed in megakaryocytes from PMF patients. *Gata1^{low}* megakaryocytes express the same maturation abnormalities, including retarded maturation, high levels of TGF-β and P-selectin expression and increased emperipolesis with neutrophils, than those expressed by megakaryocytes from PMF patients [13, 15]. It is not surprising then that with age, CD1 *Gata1^{low}* mice develop all the traits associated with PMF [32]. By contrast with other animal models that develop myelofibrosis secondary to other myeloproliferative neoplasms [33, 34], *Gata1^{low}* mice develop a phenotype resembling primary myelofibrosis as an orderly sequence of events which allow deconstruction of the complex traits of the disease [32]. *Gata1^{low}* mice remain fibrosis-free up to 5-6-months, became fibrotic by 6-10-months and develop all the disease markers, including extramedullary hematopoiesis in liver, by 17-months [32]. The pathogenetic role of TGF-β in this animal model is supported by the observations that *Gata1^{low}* mice are cured by treatment with the TGF-β receptor 1 kinase (ALK5) inhibitor SB431542 [15] and that their bone marrow and spleen express distinctive abnormalities of TGF-β signaling profiling similar to those characterizing these organs in PMF patients [15, 35]. However, as in the case of PMF patients, the levels of TGF-β in plasma and organ washes of these mice are only modestly greater (by 2-fold) than normal [15]. Whether, in these mice, and possibly in PMF patients, fibrosis may provide a substrate that increases TGF-β bioavailability in the microenvironment is un known.

The aim of this study was to assess the bioavailability of TGF-β in the spleen from *Gata1^{low}* mice during disease progression and to identify possible pathological cell interactions of the megakaryocytes, in addition to the emperipolesis with neutrophils already described, that may alter TGF-β bioavailability in myelofibrosis. To address this aim, we performed extensive immune-histological and immune-transmission electron microscopy (TEM) observations of spleens from *Gata1^{low}* mice at 3-, 6-10- and 17-months of age. Mechanistic insights in support of these snap-shot observations were obtained by performing similar studies on *Gata1^{low}* mice lacking TGF-β or P-selectin functions.

Materials and methods

Human subjects

Spleen samples from 6 patients with PMF were kindly provided by Dr. Gianni Barosi (Policlinico San Matteo, Pavia, Italy). Diagnoses were established according to WHO criteria [36]. Specimens were collected according to guidelines established by the local ethical committees for human subject studies and after written informed consent had been obtained in accordance with the 1975 Helsinki Declaration revised in 2000.

Mice

Male wild-type and *Gata1^{low}* mice were generated in the animal facility of Istituto Superiore di Sanità as described [31, 32]. The mutant mice were divided into three age groups that correspond to specific stages of disease progression: disease-free (3-months old), early-myelofibrotic (6-10 months), when presence of the disease is detectable only in bone marrow, and myelofibrotic (>15-months), when the complete clinical picture of the human disease is manifested [32]. Double *Gata1^{low} pSel$^{null/null}$* males were generated according standard genetic protocols started by crossing *Gata1$^{low/low}$* females with *p-Sel$^{null/null}$* males provided by Dr. Frenette (Albert Einstein University, New York, NY) [37]. Control experiments were performed on age matched littermates, as indicated. All the experiments were performed according to protocols approved by the institutional animal care committee according to the European Directive 86/609/EEC.

Pharmacological inhibition of TGF-β treatment

SB431542 (cat no S4317-5GM, ID_{50} for AKL5 = 94 nM, Sigma-Aldrich, St Louis, MO, USA) was dissolved in dimethyl sulphoxide (10 mg/mL, Sigma) and diluted to a concentration of 60 mg/mL with phosphate buffer saline. 12-months old *Gata1^{low}* mice were divided into 2 groups which were injected intraperitoneally with either SB431542 (60 μg/day) or vehicle for 2 cycles of 5 consecutive days two days apart, left untreated for 1 month and then treated for 2 additional cycles as described [15]. Mice were sacrificed three days after the last day of treatment.

Histology

Spleens were fixed in 10% (v/v) phosphate-buffered formalin according to standard procedures. Once fixed, tissues were paraffin embedded and cut into consecutive 2.5-3 μm sections that were then stained either with Gomori-silver (MicroStain MicroKit, Bologna, Italy), Mallory Trichromic and Wiegert Van Gieson (both from Bio-Optica, Milan, Italy) staining [38-40]. Microscopic evaluations were performed with a DM RB microscope (Leica LTD, Heidelberg, Germany) set in a trans-illumination mode and images acquired with the IM 50 system (Leica). The frequency of megakaryocytes, neutrophils and fibrocytes was determined in randomly chosen multiple sections to cover a total area of 33.5 mm^2.

Immuno-histochemistry

Consecutive sections of 4-6 μm were cut from paraffin embedded spleen samples and incubated either with anti-TGF-β (sc-146, Santa Cruz Biotechnology, Santa Cruz, CA), anti-collagen type I (AB765P) or anti-fibronectin (F7387) monoclonal antibodies (both from Sigma, Milan, Italy). Staining was revealed by an avidin-biotin immuno-peroxidase system (Vectastain Elite ABC Kit; Vector laboratories, Burlingame, CA, USA), as described by the manufacturers. Samples not incubated with the primary antibody or incubated with a non-immune IgG served as negative controls. Samples were counterstained with Hematoxylin-eosin and analyzed with a light microscope (Leica) equipped with a Coolsnap videocamera for computerized images (RS Photometrics, Tucson, AZ, USA).

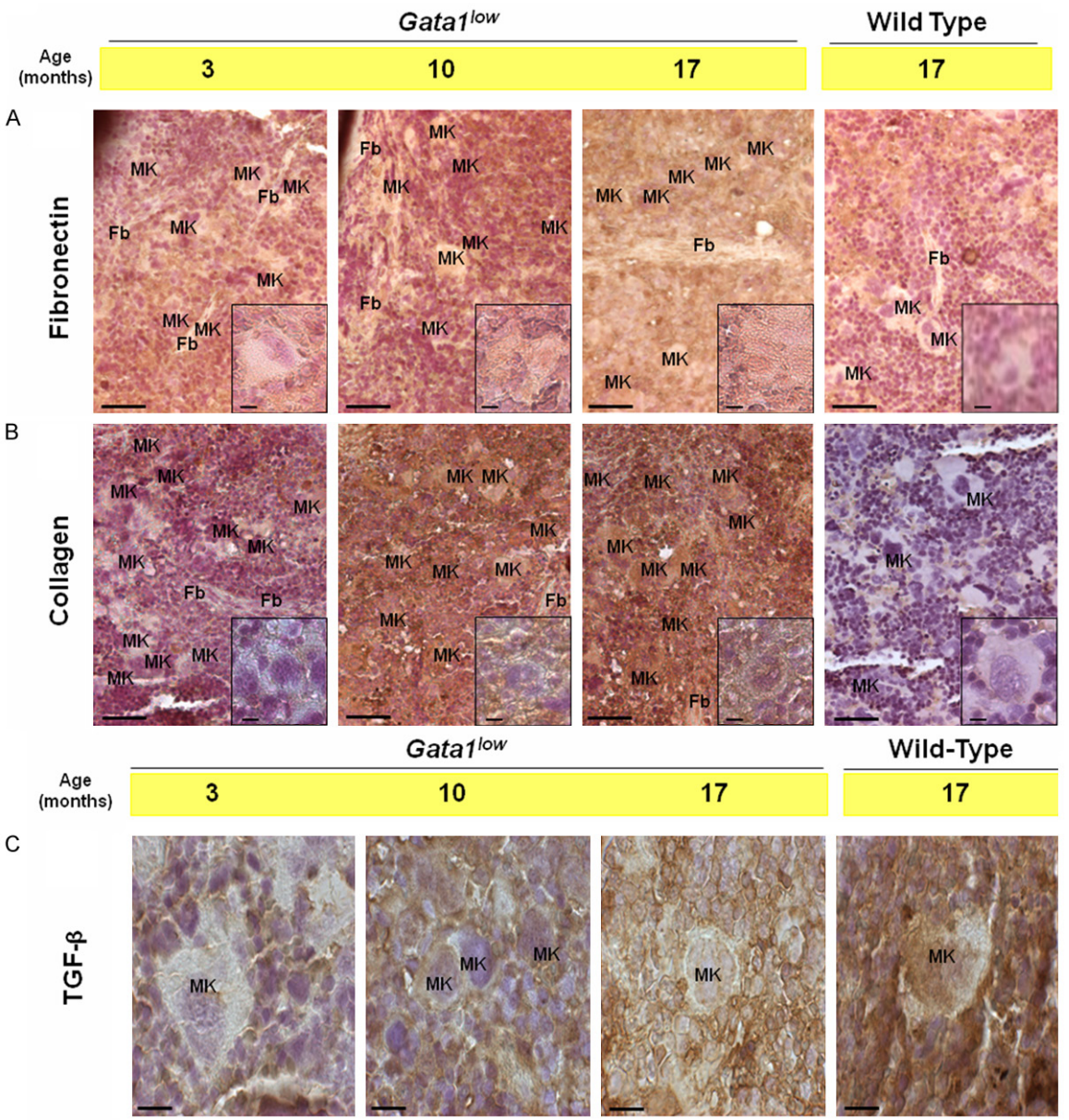

Figure 1. *Progressive accumulation of fibronectin, collagen and TGF-β in the spleen from Gata1^{low} mice with disease progression.* Immuno-histochemistry for fibronectin (A), collagen (B) and TGF-β (C) of consecutive spleen sections from progressively older *Gata1^{low}* mice, as indicated. Representative sections from the spleen of a 17-months old wild-type animal were processed in parallel, for comparison. Aging is associated with progressive increases in immuno-staining for fibronectin, collagen and TGF-β. As shown in the inserts, fibronectin and collagen staining is localized in areas surrounding megakaryocytes. TGF-β staining is localized both in megakaryocytes and in extracellular areas. To be noted the strong staining of the megakaryocyte from 17-months wild-type littermates. The spleen of these animals, however, contained few megakaryocytes. Legend: Fb = fibrocyte; MK = megakaryocytes. Magnifications 40x in panels (A, B) and 100x in panel (C) and in the inserts in (A, B). Scale bars indicate 20 mm in panels (A, B) and 10 mm in their inserts and 10 mm in panel (C).

Transmission electron microscopy (TEM)

Spleens were fixed in 2.5% glutaraldehyde in 0.1 M cacodylate buffer, pH 7.6, for 2 hours at 4°C and post-fixed in osmium tetroxide for 60 min at 4°C (all from Sigma) according to standard procedures [13, 15]. The samples were then dehydrated in alcohol at progressively higher concentrations and embedded in Spurr resin (Poliscience, Warrington, PA). Consecutive thin and ultrathin sections were cut using a Reichert ultramicrotome (Depew, NY, USA).

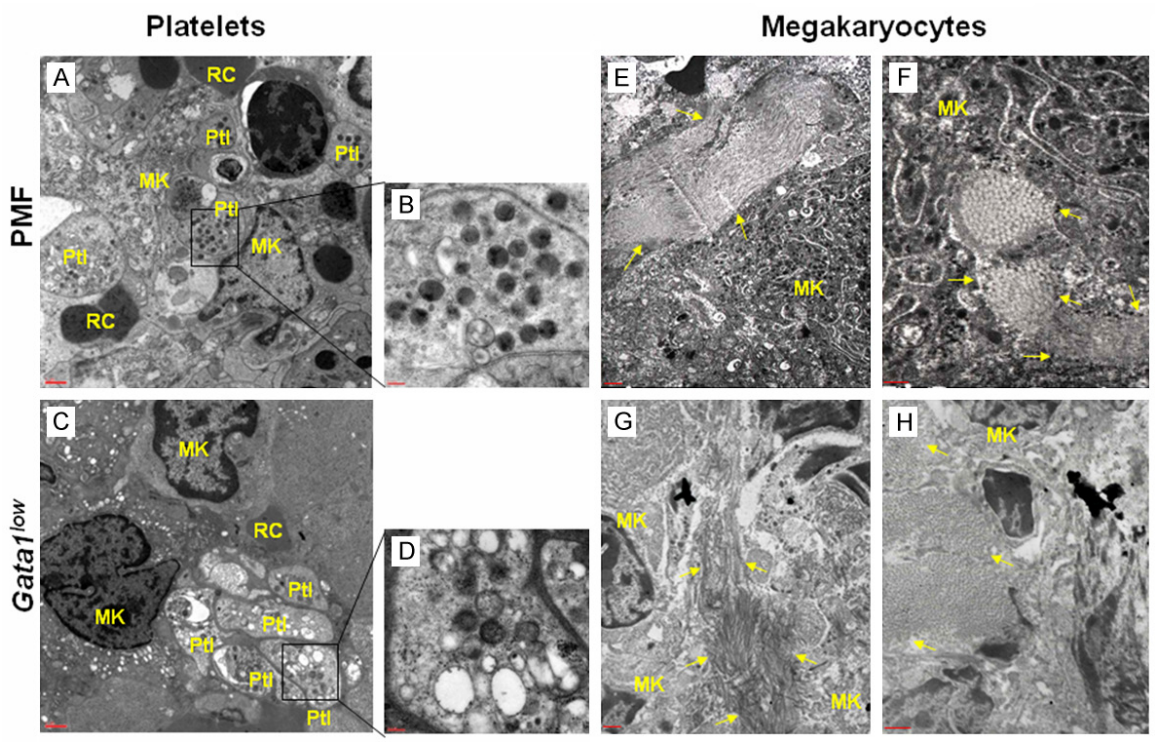

Figure 2. *Numerous megakaryocytes from the spleen of both PMF patients and Gata1^{low} mice present collagen fibres embedded in their cytoplasm.* Megakaryocyte maturation is similarly impaired in PMF patients (top panels) and *Gata1^{low}* mice (bottom panels). In fact, TEM observations confirmed that both PMF and *Gata1^{low}* platelets are larger than normal (megathrombocytes, average diameter = 3.5 mm vs 1.9 mm expected for normal platelets) and contain excessive endoplasmic reticulum and reduced numbers of a-granules, which remain light electron-dense, and other organelles (A-D) [5, 13]. Megakaryocytes are mostly immature, as indicated by their smaller size and poorly developed DMS and platelet territories (E-H) [5, 13]. Surprisingly, we identified that many megakaryocytes present in the spleen of PMF patients and *Gata1^{low}* mice contained fibres with the distinctive TEM appearance of mature collagen polymers in their cytoplasm (E-H). The arrows in (E, G and F, H) indicate examples of longitudinal and cross sections of collagen fibres within the megakaryocyte cytoplasm. Results are representative of observations made on spleens from six PMF patients and three *Gata1^{low}* mice, respectively. Legend: Ptl = platelets, RC = red cell, MK = megakaryocyte, arrow = collagen fibres. Magnifications 4,400x in (A, C and E, G); 7,000x in (H); 12,000x in (F); and 30,000x in (B, D), respectively. Scale bars indicate either 2 mm (A, C, E, G, H) or 0.5 mm (F) or 0.2 mm (B, D).

Semithin section were stained with Methylenblue, for morphological analysis, while ultrathin sections were collected on 200 mesh copper grids, counterstained with uranyl acetate and lead citrate and observed with an EM 109 Zeiss (Oberkochen, Germany). Images acquired with the AXIOSKOPE microscope (ZEISS, Jena, Germany) equipped with a CooIsnap Videocamera were quantified with the MetaMorph 6.1 Software (Universal Imaging Corp, Downingtown, PA, USA). Quantitative determinations were performed on a minimum of 50 cells per experimental point and each experiment was repeated on spleens obtained from at least 3 separate mice per experimental group.

Immuno-TEM

Spleens were fixed for 3 hours at 4°C in a mixture of 2% paraformaldehyde and 0.1% glutaraldehyde in 0.1 M cacodylate buffer, pH 7.6, dehydrated in alcohol at progressively higher concentrations and embedded in Bioacryl resin (British Biocell, Cardiff, United Kingdom), followed by UV polymerization, according to standard procedures (13). Ultrathin sections were cut and mounted on 300 mesh nickel grids. To block non-specific binding sites, these grids were treated with a blocking buffer made of phosphate buffer saline supplemented with 0.1% Tween-20, 0.1% bovine serum albumin and 4% normal rabbit serum, and incubated overnight in the presence of anti-TGF-β, anti-

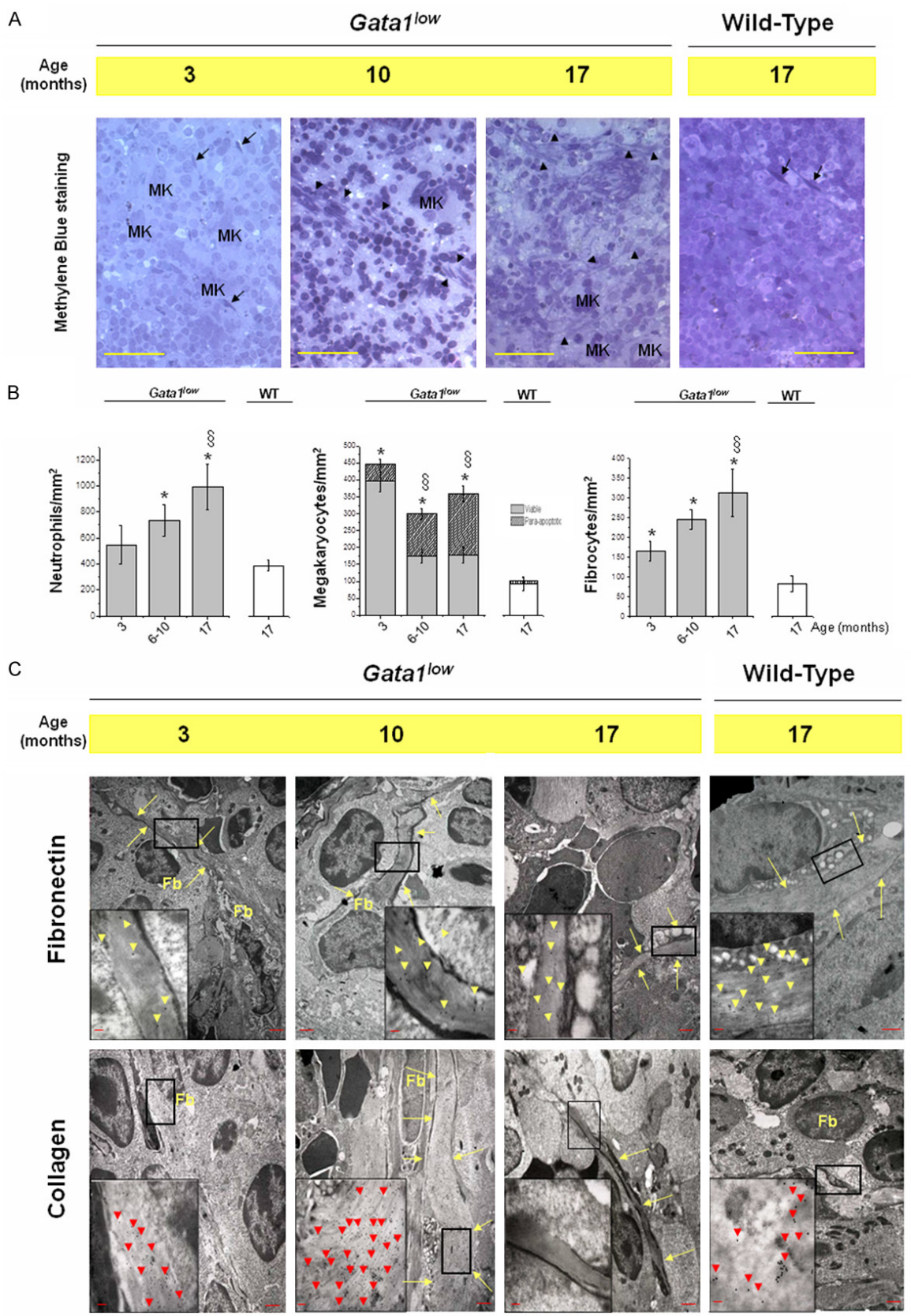
A
Gata1low
Wild-Type
Age (months)
3
10
17
17
Methylene Blue staining
MK
B
Gata1low
WT
Neutrophils/mm2
Megakaryocytes/mm2
Viable
Para-apoptotic
Fibrocytes/mm2
3
6-10
17
Age (months)
C
Gata1low
Wild-Type
Age (months)
3
10
17
17
Fibronectin
Collagen
Fb

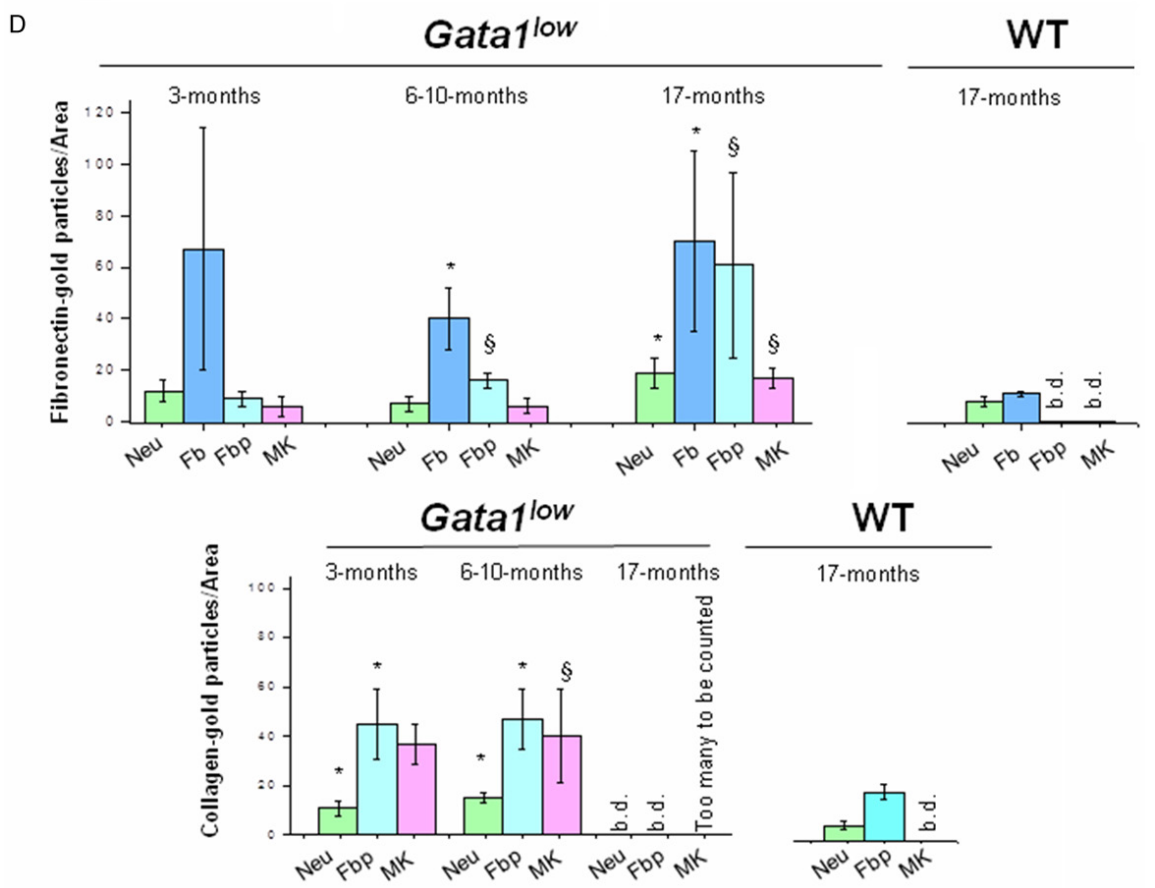

Figure 3. *Increased frequency of activated fibrocytes in spleen sections from Gata1^{low} mice during disease progression.* A. Methylene Blue staining of semithin sections from the spleen of representative *Gata1^{low}* mice of increasing age, as indicated. 17-months old wild-type littermates were analyzed as controls. Individual fibrocyte-like cells are already detectable in the spleen from young (3-months) *Gata1^{low}* mice (arrows) and are localized close to megakaryocytes. With disease progression (10- and 17-months), fibrocyte-like cells increase in frequency forming clusters surrounding individual megakaryocytes (arrowheads). Both megakaryocytes and fibrocyte-like cells are rare in the spleen of 17-months old wild-type littermates. Legend: MK = megakaryocyte; arrow and arrowhead = individual and clusters of fibrocyte-like cells, respectively. Magnifications 20x. Scale bars indicate 50 mm. B. Frequency of neutrophils, megakaryocytes and fibrocytes in spleen sections from *Gata1^{low}* mice during disease progression. Values obtained with 17-months old animals wild-type at the *Gata1^{low}* locus are reported for comparison. Megakaryocytes were divided into viable and para-apoptotic according to the appearance of their nuclei (nuclei with both euchromatic and heterocromatic regions or with heavily heterochromatic regions only). Results are presented as Mean (±SD) of observations performed with at least three mice per experimental group. * and § indicate values statistically significant ($p<0.05$ by Anova) with respect to those observed in wild-type and 3-months old *Gata1^{low}* mice. C. Immuno-TEM for fibronectin (top panels) and collagen (bottom panels) of representative fibrocytes from 3, 10 and 17-months old *Gata1^{low}* mice, as indicated. Representative cells from a 17-months old wild-type mouse are presented as control. Rectangles indicate areas of the fibrocyte protrusions (indicated by arrows) shown at greater magnification in the inserts. In 17-months old *Gata1^{low}* mice, fibrocyte protrusions were no longer positive for collagen. Legend: Fb = fibrocyte, yellow arrows = fibrocyte protusion, yellow and red arrowheads = fibronectin- and collagen-related immuno-gold particles, respectively. The results are representative of those obtained with at least three mice per experimental group. Magnifications 4,400x in the panels and 30,000x in the inserts. Scale bars indicate 2 mm in the panels and 0.2 mm in the inserts. D. Quantification of immuno-gold staining for fibronectin (top panels) and collagen (bottom panels) of neutrophils (Neu), fibrocytes (Fb), fibrocyte protusions (Fbp) and megakaryocytes (MK) from the spleen of *Gata1^{low}* mice during disease progression. Values observed with 17-months old wild-type mice are reported for comparison. In the case of neutrophils and activated fibrocytes, results are expressed as numbers of gold particles per cell. In the case of fibrocyte protrusions and megakaryocytes, results are expressed as numbers of gold particle per area of observation (14 μm^2). Results are presented as Mean (±SD) determinations of at least 5 cells per mouse with three mice per experimental group. * and § indicate values statistically significant ($p<0.05$ by Anova) with respect to those observed in wild-type and 3-months old *Gata1^{low}* mice, respectively. bd = below detection.

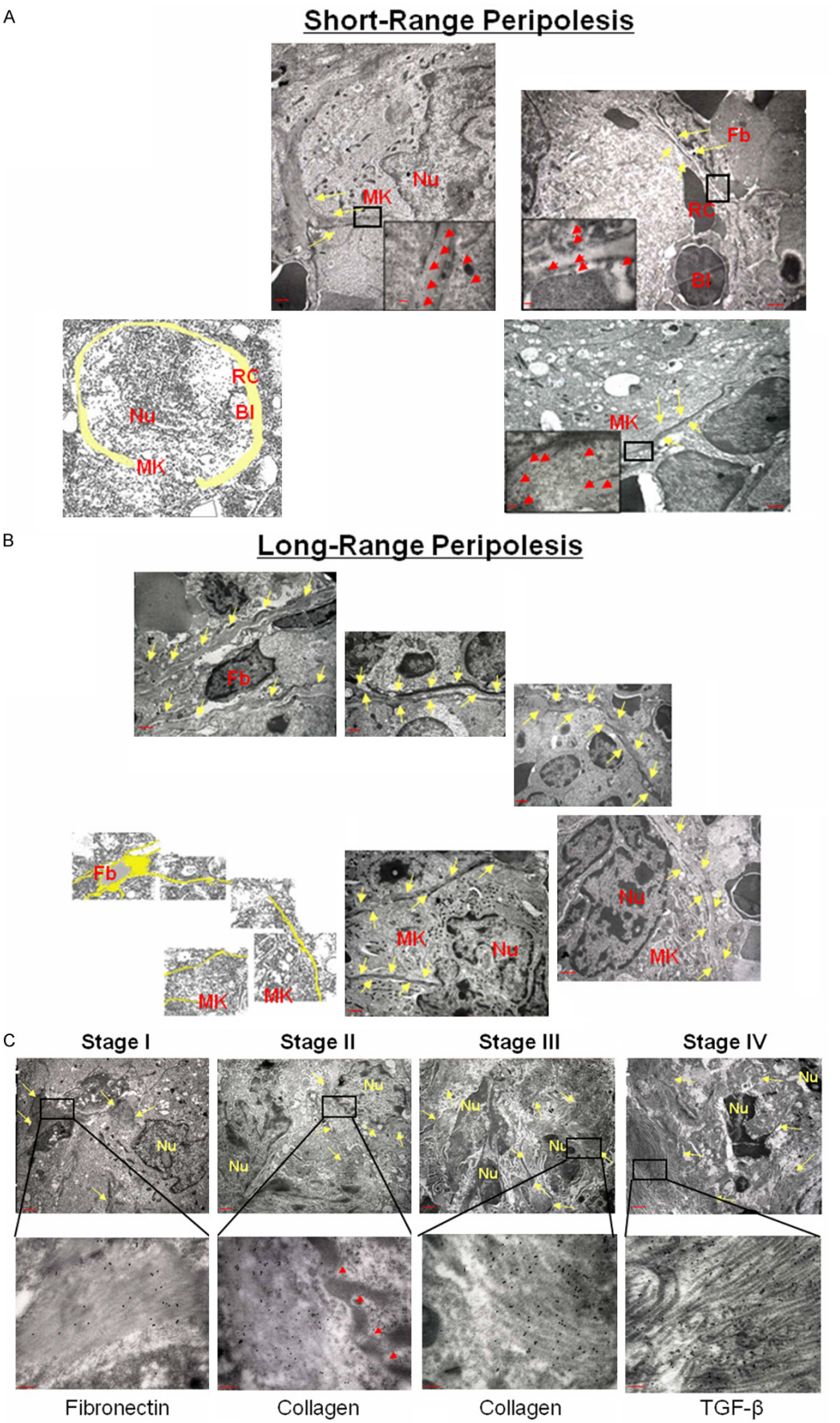
A
Short-Range Peripolesis
Nu
MK
Fb
RC
Bl
RC
Nu
Bl
MK
MK
B
Long-Range Peripolesis
Fb
Fb
MK
MK
MK
Nu
Nu
MK
C
Stage I
Stage II
Stage III
Stage IV
Nu
Nu
Nu
Nu
Nu
Nu
Nu
Nu
Fibronectin
Collagen
Collagen
TGF-β

Figure 4. *Peripolesis of an activated fibrocyte around a megakaryocyte, a novel cell interaction observed in the spleen of Gata1^{low} mice.* A. Representative short-range peripolesis. An activated fibrocyte (Fb) surroundings with its protrusions (positively identified by the collagen staining presented in the insert) a megakaryocyte (recognized by the presence of platelet territories in its cytoplasm) and intruding at least three of its protrusions in the megakaryocyte cytoplasm. Of note, the collagen-specific gold particles are localized not only in the protrusions but also in the cytoplasm of the megakaryocyte. In this particular case a red cell and a blast-like cell were also embedded in the megakaryocyte cytoplasm. These events were however extremely rare. Three TEM photographs were assembled together to cover portions of the megakaryocyte cytoplasm sufficiently vast to let appreciate the relative size of the cells and the length of the fibrocyte protrusions. A computer generated image is presented to help with the identification of the different structures. B. Representative long-range peripolesis. The fibrocyte has developed more than one protrusion, indicated by arrows in the first panel on the top. One of these expanded over several photographic areas infiltrating itself through other cells, until reached a megakaryocyte. It surrounded the megakaryocyte and infiltrated its cytoplasm. A computer generated reconstruction is included for convenience. Legend: Fb = fibrocyte, MK = megakaryocyte, Nu = nucleus, RC = red cell, Bl = blast. Protrusions are indicated by yellow arrows, immunogold particles for collagen by red arrowheads. Ultrastructural details of the fibrocyte protrusions are presented in the inserts. C. Progressive changes in the immuno-TEM appearance of megakaryocytes and protrusions of activated fibrocytes associated in peripolesis. The top and bottom panels present representative immuno-TEM images of megakaryocytes at four stages of fibrocyte peripolesis and of the protrusions embedded in their cytoplasm. The megakaryocytes were immuno-stained with antibodies for fibronectin, collagen and TGF-β, as indicated. To be noted the para-apoptotic features of the nuclei of megakaryocytes at stage III and IV of peripolesis and the great TGF-β content of those at stage IV. Further morphological details are described in the text. Legend: Nu = nucleus; arrows = fibrocyte protrusion; red arrowheads = leaks in the membrane of the fibrocyte protusion. Magnifications 4,400x and 30,000x in the panels and inserts, respectively. Scale bars indicate 2 mm in the panels and 0.2 mm in the inserts.

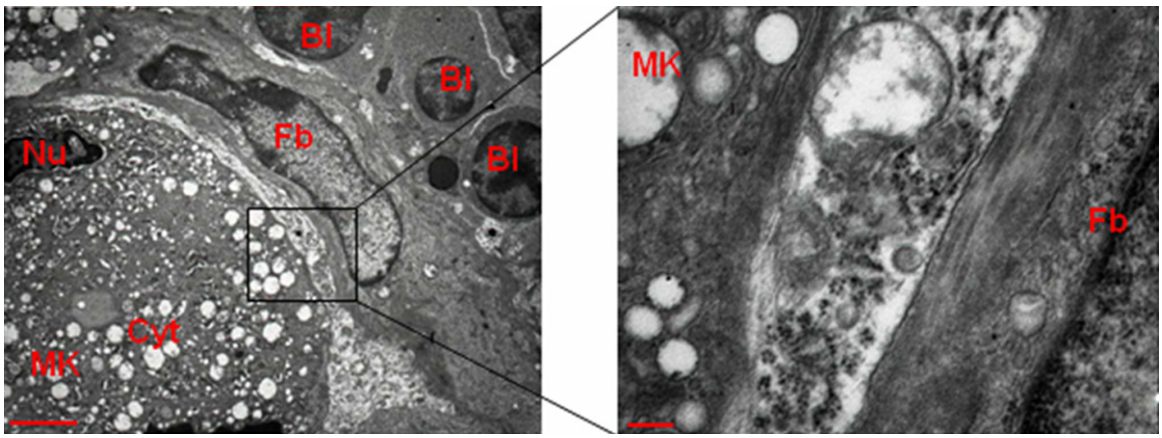

Figure 5. *Details of a short-range peripolesis between an activated fibrocyte and a megakaryocyte showing that the two cells remain separated by an extracellular space filled with structured electron-dense material.* The rectangle on the left panel indicates the area of shown at greater magnification on the right. Legend: Bl = blasts; Cyt = cytoplasm; Fb = fibrocyte; MK = megakaryocyte; Nu = nucleus. Magnifications 4,400x and 30,000x in the left and right panel, respectively. Scale bars indicate 2 μm in the left panel and 1 μm in the right panel.

fibronectin, anti-collagen type I and anti-myeloperoxidase (sc-16128, Santa Cruz) antibodies. The grids were then incubated for 1 hour with rabbit anti-goat IgG conjugated with 15 nm collaidal-gold particles (British Biocell, Cardiff, United Kingdom), counterstained in uranyl acetate to evidentiate the cell morphology, and observed with EM 109 Zeiss. In co-localization experiments, secondary antibodies were coupled with either 10 or 20 nm gold particles (always from British Biocell). Negative controls were represented by cells treated as above, but not exposed to the primary antibody. Semiquantitative observations were obtained on 20-50 individual cells. Twenty-fifty cells were visually analyzed for each experimental point and the number of immuno-gold particles counted by eye at 30,000 x magnification in 5 randomly selected cells.

Statistical analysis

Results are presented as the mean (±SD) of three separate experiments and statistical analysis was performed by analysis of variance (Anova test) using Origin 3.5 software for

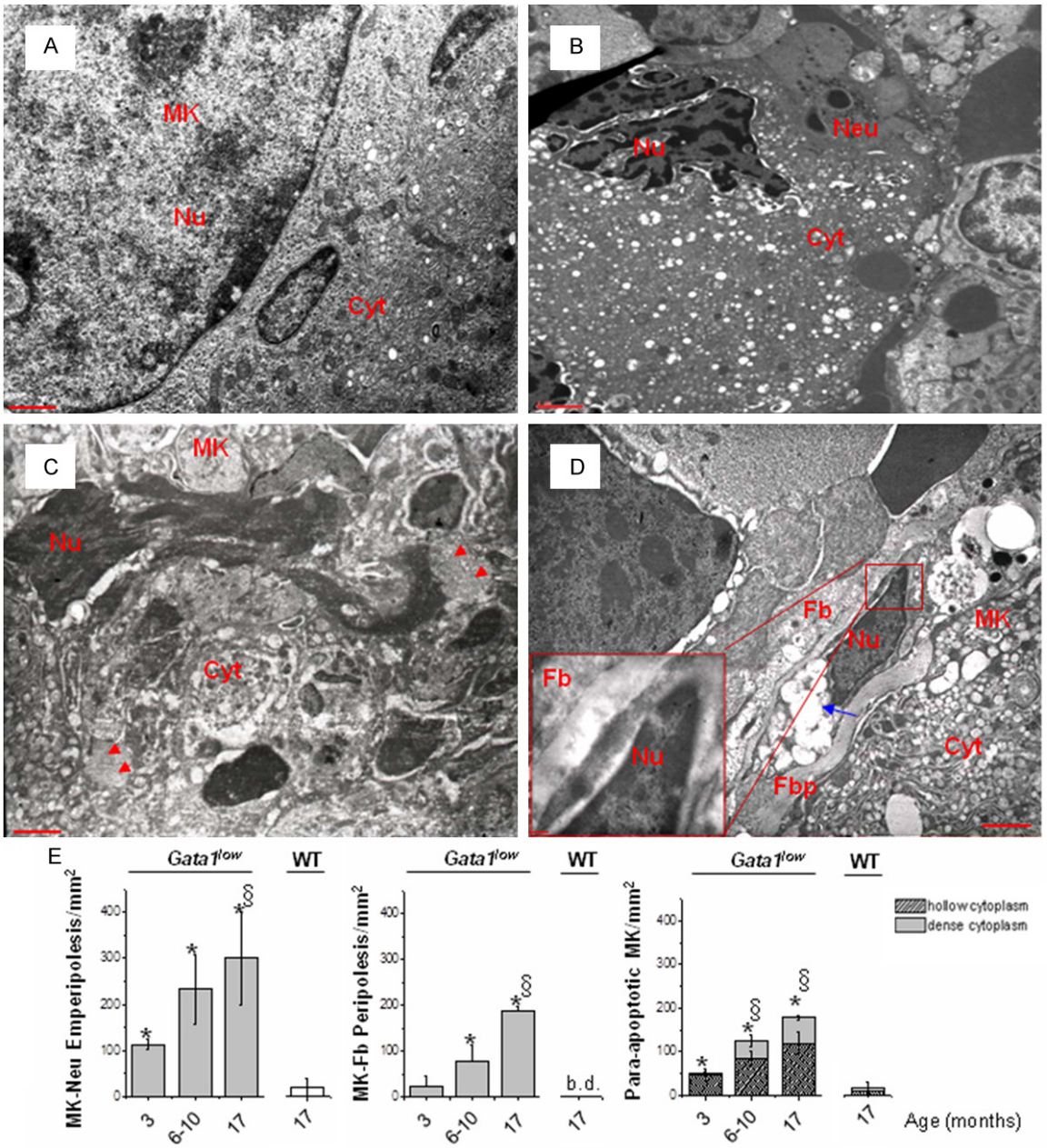

Figure 6. *Para-apoptosis with electron-dense cytoplasm is a novel process of cell death occurring in megakaryocytes from the spleen of Gata1^{low} mice.* (A-D) Representative TEM images of a viable megakaryocyte (A) and of two megakaryocytes the nuclei of which present the tightly condensed chromatin features characteristic of para-apoptotic cells (B, C). In (B), the cytoplasm of the para-apoptotic megakaryocyte has a vacuolated structure (electron-hollow) and is emperipolesed by a neutrophil. In (C), the cytoplasm of the para-apoptotic megakaryocyte has a disorganised electron dense appearance (electron-dense) that does not allow recognition of any of its structures (endoplasmic reticulum, DMS or platelet territories). (D) Representative TEM of an activated fibrocyte establishing peripolesis with a megakaryocyte and undergoing electron-hollow para-apoptosis (see the characteristic electron-light vesicles in its cytoplasm and the electron-density of its nucleus, shown at greater magnification in the insert). Legend: Cyt = cytoplasm, Nu = nuclei, Neu = neutrophil; Fb = activated fibrocytes; Fbp = fibrocyte protusions; MK = megakaryocyte; arrowheads = collagen fibres; blue arrow = electron-light vesicles. Magnifications correspond to 4,400x in the panels and 30,000 in the inserts. Scale bars indicate 2 mm length in the panels and 0.2 mm length in the inserts. (E) Quantification of the frequency of emperipolesis between megakaryocytes and neutrophils (left panel), of peripolesis between megakaryocytes and activated fibrocytes (middle panel), and of para-apoptotic megakaryocytes (with electron-dense or electron-hollow cytoplasm) (right panel) occurring in the spleen of *Gata1^{low}* mice with disease progression. Values observed with 17-months old wild-type mice are reported for comparison. Results are presented as Mean (±SD) determinations of at least three mice per experimental group. * and § indicate values statistically significant ($p<0.05$ by Anova) with respect to those observed in wild-type and 3-months old *Gata1^{low}* mice, respectively. bd = below detection.

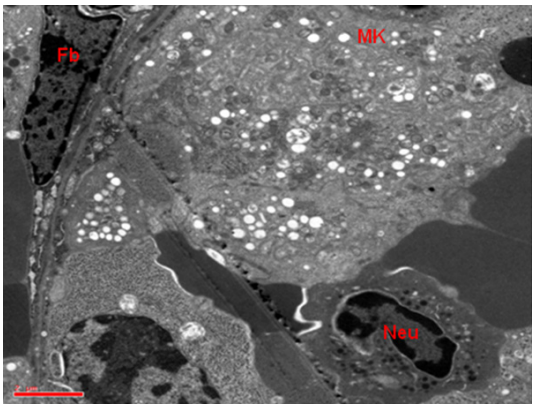

Figure 7. *Representative megakaryocyte engaged both in emperipolesis with a neutrophil and in peripolesis with an activated fibrocyte.* Legend: Fb = fibrocyte; MK = megakaryocyte; Neu = Neutrophil. Magnification 4,400x. Scale bar indicates 2 μm.

Windows (Microcal Software Inc., Northampton, MA).

Results

Numerous megakaryocytes from the spleen of PMF patients and Gata1^{low} mice contain collagen fibres embedded in their cytoplasm

During disease progression, fibrosis is observed not only in the marrow but also in the spleen of *Gata1^{low}* mice, as well as in that from PMF patients [15]. Fibronectin and collagen immuno-staining of consecutive spleen sections from *Gata1^{low}* mice (**Figure 1A** and **1B**) and PMF patients (data not shown) indicated that fibrosis is localized in areas surrounding and including megakaryocyte clusters, confirming that these cells participate in the development of fibrosis. Megakaryocytes are thought to play a passive role in this process by releasing in the microenvironment TGF-β [13], the growth factor which activates fibrocytes to produce collagen [24], and lysyl oxidase 2 (LOX2), the enzyme that catalyse the polymerization reaction necessary to form mature collagen fibres [41] which is expressed at abnormally high levels in *Gata1^{low}* megakaryocytes [42]. By contrast with this hypothesis, immuno-TEM observations revealed that the cytoplasm of numerous megakaryocytes from the spleen of PMF patients and *Gata1^{low}* mice presents, in addition to the ultra-structural abnormalities associated with retarded maturation which are the hallmark of the disease [5, 7, 13], fibres with ultrastructural features characteristic of mature collagen polymers (**Figure 2**). Mature collagen fibres have a distinctive TEM morphology characterized by a sequence of dark and light electron density bands with a periodicity of 64 nm [43]. Each string is formed by three inter-twisted polymers and light and dark bands correspond to entangled and emptied regions of the polymer braid, respectively. These ultrastructural features were observed in megakaryocytes from the spleen of PMF patients and *Gata1^{low}* mice (**Figure 2**) but not in those from non-diseased individuals or wild-type mice (not shown). The frequent presence of mature collagen fibres within the megakaryocyte cytoplasm suggested to us that these cells may exert an active role in the development of fibrosis. This hypothesis was tested by performing immune-histochemistry and immuno-TEM studies of the spleen during disease progression of *Gata1^{low}* mice.

The spleen from Gata1^{low} mice contains increased numbers of neutrophils, megakaryocytes and activated fibrocytes

The spleen is the main hematopoietic site of *Gata1^{low}* mice [44]. It is therefore not surprising that semithin sections of spleen from these animals contained increased numbers of hematopoietic precursors of all types including neutrophils (2-fold) and megakaryocytes (4-fold) (**Figure 3A**, **3B** and data not shown). In addition, these observations revealed the presence of numerous cells with the morphology of activated fibrocytes localized in clusters in proximity of megakaryocytes, the frequency of which increased by 2-3-fold during disease progression (from 165±26/mm^2 at 3-months to 312±60 at 17-months) (**Figure 3A**, **3B**). Immuno-TEM investigations identified that these cells were indeed activated fibrocytes containing 2-4 protrusions each, with an average length of 1,145 ± 832 nm. In one case in which we were able to follow the same protrusion in multiple fields, we determined that its total length reached 2,500 nm (data not shown). These cells expressed high levels of fibronectin and collagen (**Figure 3C**, **3D**). By contrast, fibrocyte-like cells were barely detectable in semithin-sections of spleen from young wild-type mice and were present with a frequency of 80±20/mm^2 on spleen sections from 17-months old wild-type mice (**Figure 3A**, **3B** and results not

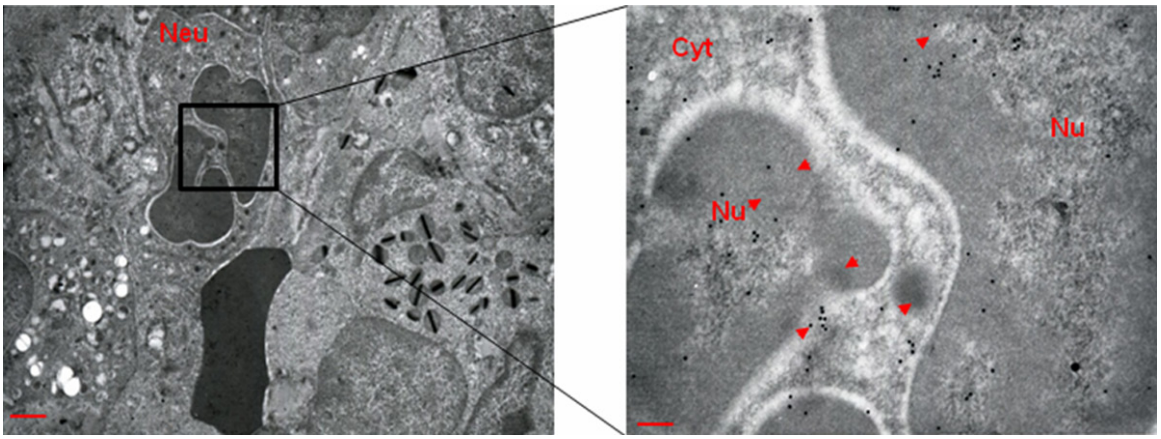

Figure 8. *Immno-TEM for TGF-β of a representative neutrophil from the spleen of a 10-month old Gata1^{low} mouse.* The rectangle on the left panel indicates the area of shown at greater magnification on the right. Legend: Cyt = cytoplasm; Neu = neutrophil; Nu = nucleus, arrowheads = TGF-β-gold particles. Magnifications 4,400x and 30,000x in the left and right panel. Scale bars indicate 2 mm and 0.2 mm in the left panel and right panel.

shown). These cells contained only 1-2 short protrusions (average length 2.32 nm) and expressed barely detectable levels of fibronectin and collagen (**Figure 3C**, **3D**). These observations suggest that the few fibrocytes detected in spleen from wild-type mice are not activated.

Quantitative determinations of the frequency of fibronectin and collagen-gold particles present in the various cell types from the spleen during disease progression of *Gata1^{low}* mice were performed (**Figure 3D**). At 3-months of age, fibronectin-gold particles were detected in the cytoplasm (67±47 gold particles/cell) rather than in the protrusions (9±3 gold particles/14 μm) of a minority (~30%) of activated fibrocytes. With disease progression, fibronectin-gold particles were detected in 100% of activated fibrocytes and their numbers remained constant in the cytoplasm (~40-70 particles/cells) and increased up to 61±36 gold particles/14 μm^2 in the protrusions. The pattern of collagen immuno-gold staining was partially different from that of fibronectin. At 3-10-months of age, high numbers of collagen-gold particles (45±14 gold particles/14 μm^2) were detected in the protrusions of all activated fibrocytes analyzed but were barely detectable in their cytoplasm (**Figure 3D** and results not shown). At 17-months, collagen-gold particles became undetectable also in the protrusions. Of note, only 30% of the fibrocytes from the spleen of 17-months old wild-type mice contained few fibronectin (11±1/cell)- and collagen (13±2/cell)-gold particles.

Activated fibrocytes were not the only cells in the spleen of *Gata1^{low}* mice that reacted with the fibronectin and collagen antibodies. While gold particles were never detected in red cells (data not shown), they were detectable in neutrophils (12-19 fibronectin-gold particles/cells and 11-15 collagen-gold particles/cells) and in megakaryocytes (**Figure 3D**). In megakaryocytes, the fibronectin-gold particles modestly increased with age (6 vs 17 fibronectin-gold particle/14 μm^2) while those for collagen increased from 37-40/14 μm^2 gold particles at 3-10-months to too many to be counted at 17-months (**Figure 3D**).

In conclusion, the spleen of *Gata1^{low}* mice contains numerous activated fibrocytes which express high levels of collagen and therefore are probably responsible for the fibrosis observed in this organ as disease progresses. The presence of fibronectin and collagen in the cytoplasm of other resident cell populations suggests the existence of a positive mechanism leading to transfer of extracellular material (mostly collagen) from the protrusions of activated fibrocytes to the cytoplasm of other cells (mostly megakaryocytes).

Peripolesis of activated fibrocytes with megakaryocytes, a novel cell interaction observed in spleen from Gata1^{low} mice during disease progression

Immuno-TEM observations of spleen from 10-16-months *Gata1^{low}* mice revealed a previously non described cellular interaction be-

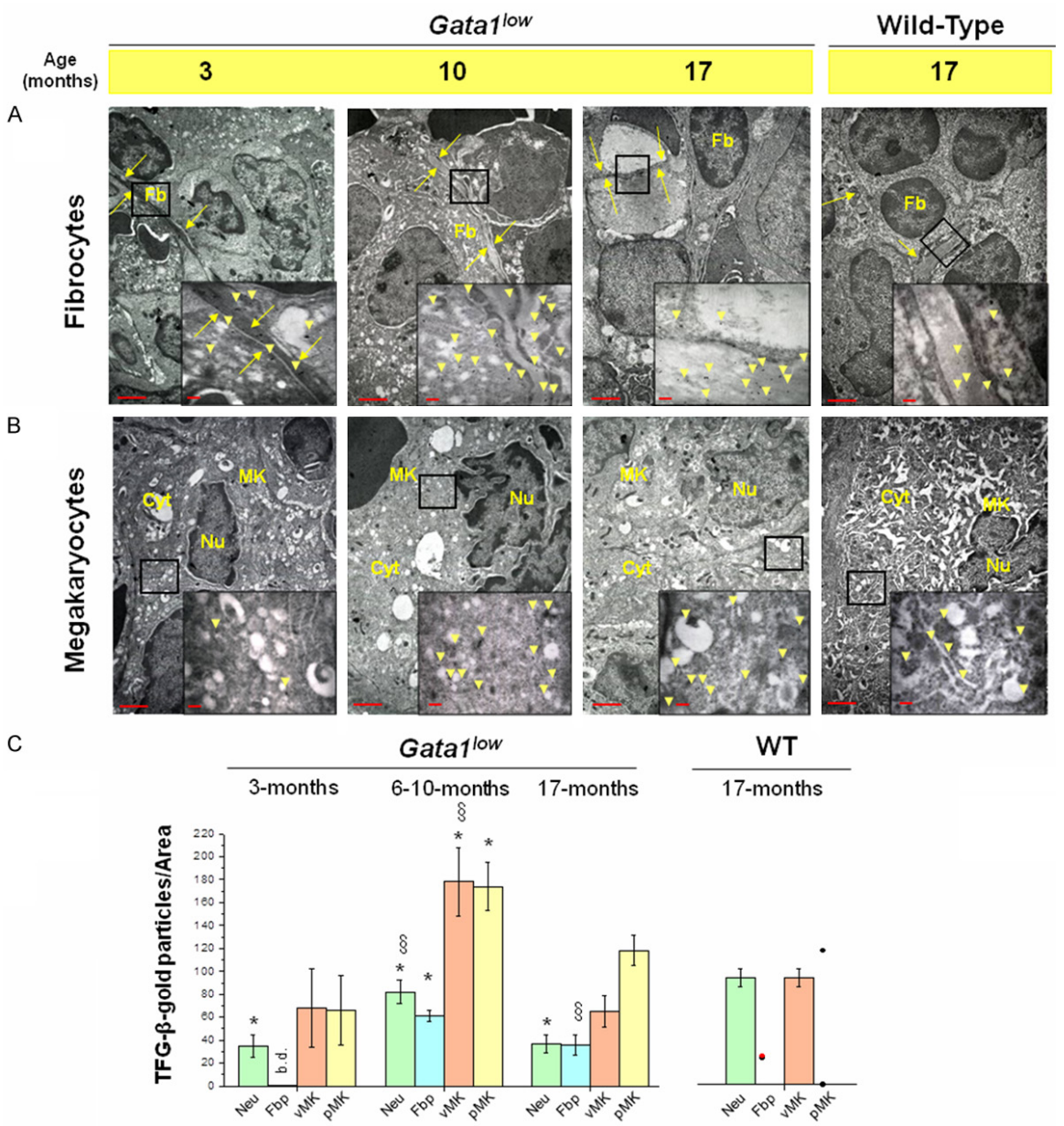

Figure 9. *Increased TGF-β content in megakaryocytes and fibrocytes in the spleen from Gata1^{low} mice during disease progression.* (A, B) Immuno-TEM for TGF-β of representative fibrocytes (A) and megakaryocytes (B) from *Gata1^{low}* mice of increasing age, as indicated. The rectangles indicate the areas of the megakaryocyte cytoplasm and of the fibrocyte protrusions (indicated by arrows) shown at greater magnification in the inserts. Representative cells from a 17-months old wild-type mouse are presented as control. The results are representative of those obtained with at least three mice per experimental group. Megakaryocytes and activated fibrocytes were recognized on the basis of their distinctive morphology. Legend: Fb = fibrocyte; MK = megakaryocyte; Cyt = cytoplasm; Nu = nucleus; arrows = fibrocyte protrusion; arrowheads = TGF-β-gold particles. Magnifications 4,400x in the panels and 30,000x in the inserts. Scale bars indicate 2 mm in the panels and 0.2 μm in the inserts. (C) Quantification of immuno-gold staining for TGF-β in neutrophils (Neu), protusions of activated fibrocytes (Fbp) and viable (vMK) or para-apoptotic (pMK) megakaryoctes from spleen sections of *Gata1^{low}* mice with disease progression. Values observed with 17-months old wild-type mice are reported for comparison. The number of TGF-β-gold particles in red cells was below detection. Results are presented as Mean (±SD) determinations of at least 5 cells per mouse with three mice per experimental group with the exception of the dots which presents the values obtained with the only 2 fibrocytes and 2 para-apoptotic megakaryocytes identified in spleens from three wild-type mice (three separate sections per mouse). * and § indicate values statistically significant ($p<0.05$ by Anova) with respect to those observed in wild-type and 3-months old *Gata1^{low}* mice, respectively. bd = below detection.

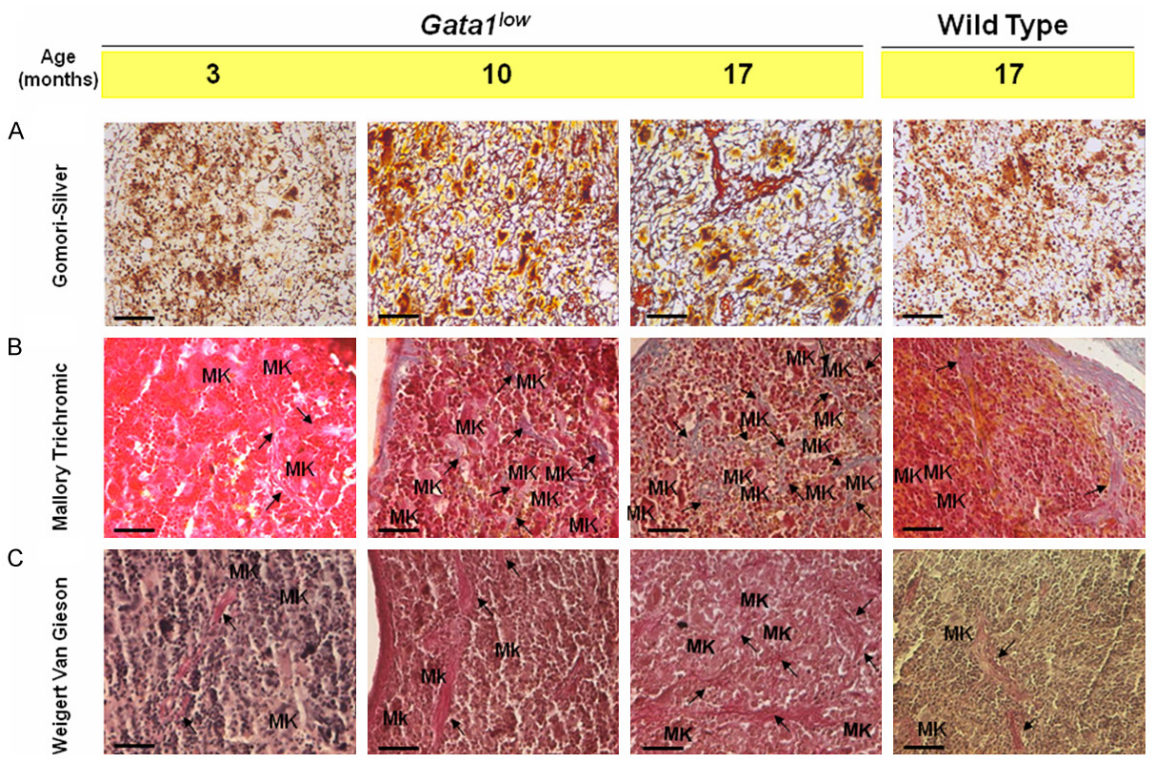

Figure 10. *Increased molecular complexity of fibrosis in spleen from Gata1^{low} mice during disease progression.* (A) Gomory-Silver, (B) Mallory Trichromic and (C) Weigert Van Geison staining of spleen sections from representative *Gata1^{low}* mice of increasing age, as indicated. 17-months old wild-type littermates were analyzed as controls. As reported [32], the extent of fibrosis increases in spleen from mutant mice with age. Gomori staining reveals the presence of reticulinic fibres in *Gata1^{low}* spleen already at 3-month. Mallory Trichromic (blue strings) and Weigert Van Geison (purple strings) staining indicate that complex collagen fibres (arrows) are detectable at 10 months and their frequency greatly increases at 17-months and are localized in areas surrounding megakaryocytes. The Weigert Van Geison staining of the spleen from 17-months old wild-type littermates reveals the presence in the extracellular area of fibres colored in yellow, an indication that they are not formed by collagen. Legend: MK = megakaryocyte; arrows = complex collagen fibres. Magnifications 40x. Scale bars indicate 20 μm.

tween activated fibrocytes and megakaryocytes (**Figure 4**). Activated fibrocytes localized in the immediate proximity of the megakaryocyte were observed to embrace these cells with their protrusions (**Figure 4A**). The main body of the two cell types remained separate by an intercellular space containing electron-dense material (**Figure 5**) while the fibrocyte protrusions established contacts so tight with the megakaryocyte that the two membranes appeared as a thickening of each other (**Figure 4A**). The protrusions appeared infiltrating the megakaryocyte cytoplasm through the DMS and, once in the cytoplasm, their presence was traceable by the presence of fibronectin and collagen-gold particles within the megakaryocyte cytoplasm (**Figure 4B** and data not shown). Fibronectin-positive protrusions were observed also within megakaryocytes apparently not surrounded by fibrocytes (**Figure 4A**). In one case we were able to trace one of these protrusions over multiple fields identifying that it originated from a fibrocyte located as far as 1,000 nm apart from the megakaryocytes (**Figure 4B**).

This novel cell-cell interaction was defined peripolesis for the greek “polesis” = center and peri = around and may also be mediated by P-selectin since this adhesion receptor has been demonstrated to mediate interaction between megakaryocytes and fibrocytes-like cells in human bone marrow [45]. We defined interactions occurring between fibrocytes and megakaryocytes in close contact with each other as short-range and that occurring between cells further apart as long-range. Most of the additional observations described below were performed on cells engaged in short-range peripolesis.

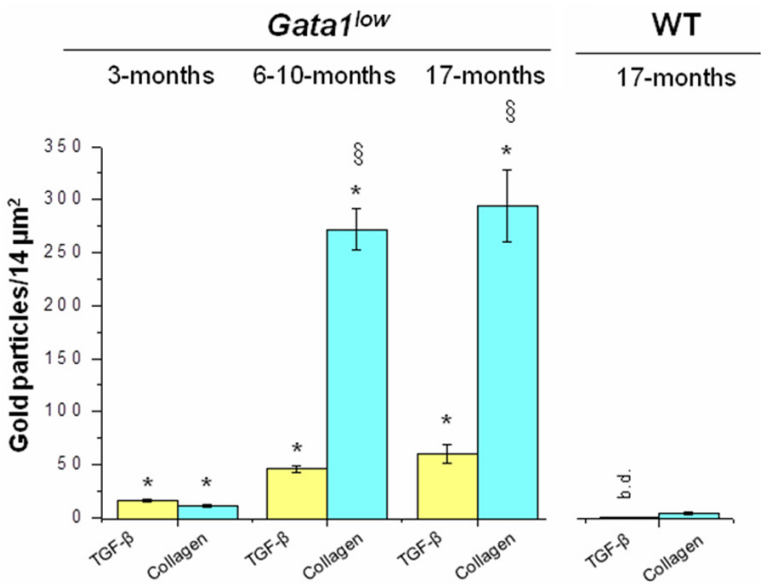

Figure 11. *The number of collagen-gold particles in the extracellular areas of the spleen from Gata1^{low} mice increases with disease progression.* Quantification of collagen- and TGF-β-gold particles in the extracellular space of spleen from *Gata1^{low}* mice during disease progression. Values observed with 17-months old wild-type mice are reported for comparison. In 17-months old Gata1^{low} mice, results are presented as mean of those observed in fibre-free and fibre-containing areas. On average, areas with mature collagen contained 2-times more TGF-β-gold paricles that those without (99.7±11.4 vs 44.3±2.9, $p<0.01$ by Anova). Results are expressed as number of gold particles per 14 µm^2 and are presented as Mean (±SD) determinations of at least 5 areas per mouse with three mice per experimental group. * and § indicate values statistically significant ($p<0.05$ by Anova) with respect to those observed in wild-type and 3-months old *Gata1^{low}* mice, respectively. bd = below detection.

On the basis of the percentage of commission between fibrocyte protrusions and megakaryocyte cytoplasm we distinguished 4 stages of peripolesis (**Figure 4C** and results not shown): Stage I, in which the membranes of the protrusion and those of the megakaryocyte DMS were still distinguishable and the presence of fibronectin (and collagen, not shown)-gold particles was detected only within the protrusion; Stage II, in which the membrane of the protrusion was leaked and collagen (and fibronectin-, not shown)-gold particles were observed both within the protrusion and in the nearby megakaryocyte cytoplasm; Stage III, in which the membrane of the protrusion was no longer recognized and high levels of collagen- (and fibronectin, not shown)-gold particles were detected in the megakaryocyte cytoplasm. At this stage, TEM ultrastructures specific for the polymerized form of collagen started to be identified in the cytoplasm of the megakaryocyte; and Stage IV, in which the cytoplasm of the megakaryocyte was infiltrated with large areas of mature collagen polymers which also contained numerous TGF-β-gold particles (**Figure 4C**).

The four stages of peripolesis were associated with progressive condensation of the megakaryocyte nuclei. In fact, starting from Stage II, the nuclei of the megakaryocytes became progressively more electron-dense acquiring a fully condensed morphology by Stage IV. The presence of nuclei with a uniformly electron-dense morphology suggests that Stage III and Stage IV megakaryocytes were dying by para-apoptosis, an immuno-mediated Tunel-negative form of cell death during which chromatin does not undergo degradation but is instead tightly condensed [12]. Further evidence that peripolesis with activated fibrocytes leads to megakaryocyte death is provided by the progressively disorganized morphology of their cytoplasms. The organelles (Stage I) and the DMS (Stage II) were no longer recognizable and the cytoplasm acquired high electron-dense features suggestive of protein degeneration (Stage III). By Stage IV, the extracellular membrane of the megakaryocytes was no longer recognizable and the condensed nucleus appeared surrounded by an electron-dense cytoplasmic "ghost" infiltrated by mature collagen polymers (**Figure 4C**). These electron-dense cytoplasmic features are strikingly different from the electron-hollow appearance of the cytoplasm from cells induced into para-apoptosis by neutrophils [7, 13]. This difference suggests that electron-dense cytoplasm para-apoptosis may represent a novel form of immune-mediated cell death.

The frequency of megakaryocytes undergoing para-apoptosis in the spleen from Gata1^{low} mice increases with disease progression

Para-apoptosis with hollow cytoplasm of megakaryocytes from *Gata1^{low}* mice and PMF

patients has been already described [11, 13]. In fact, these cells, embed in their cytoplasm one-two neutrophil(s) through a process of pathological emperipolesis during which neutrophils release their proteases in the megakaryocyte cytoplasm. These proteases progressively degrade the protein content of the megakaryocyte cytoplasm until it is completely dissolved and the cell may be traced as a naked condense multi-lobular nucleus [11]. The distinctive cytoplasmic features of megakaryocytes undergoing papa-apoptosis following interaction with neutrophils or activated fibrocytes allowed us to assess the relative frequency of the two interactions as wells as of the incidence of their effects during disease progression (**Figure 6A-E**).

Megakaryocytes engaged in neutrophil emperipolesis (**Figure 6B**) were detected as early as at 3-months (approximately ~100 megakaryocytes/mm^2, i.e. 25% of the ~400 megakaryocytes detected per mm^2) and their frequency increased by 2-fold (~200-300 megakaryocytes/mm^2) reaching ~80% of the total number of megakaryocytes (~180 alive and ~160 para-apoptotic/mm^2) detected in the spleen by 6-17-months (**Figure 6E**). By contrast, the number of megakaryocytes engaged in peripolesis with activated fibrocytes (**Figure 6C**) was barely detectable in the spleen of *Gata1^{low}* mice at 3-months (~24 megakaryocytes/mm^2, < 5% of the total) and their frequency increased to ~80 megakaryocytes/mm^2 (30% of the total) at 6-10-months and ~190 megakaryocytes/mm^2 (50% of the total) at 17-months (**Figure 6E**). Of note, in the spleen from 17-months wild-type littermates, interactions between megakaryocytes and neutrophils or activated fibrocytes were barely detectable (**Figure 6E**).

With disease progression, the frequencies of megakaryocyte interactions with neutrophils and activated fibrocytes were mirrored by those of para-apoptotic megakaryocytes with electron-hollow or electron-dense cytoplasm. Para-apoptotic megakaryocytes with hollow cytoplasm were detected in great numbers (approximately 48 cells/mm^2) already at 3-months and their number increased up to 120 cells/mm^2 (50% of the cells) by 17-months (**Figure 6E**). By contrast, para-apoptotic megakaryocytes with dense cytoplasm were barely detectable at 3-months but by 6-17-months months reached a frequency of 40-60 megakaryocytes/mm^2 (~25% of total) (**Figure 6E**).

The fact that at 17-months, 80% of megakaryocytes were engaged in neutrophil emperipolesis suggests that with disease progression the same megakaryocyte may engage both in neutrophil-emperipolesis and fibrocyte-peripolesis. Indeed, ~30% of megakaryocytes engaged with activated fibrocytes presented neutrophils embedded in their cytoplasm (**Figures 6D** and **7**). When this occurred, fibrocytes acquired a morphological features characterized by electron-dense nuclei and electron-hollow cytoplasm suggestive of death by para-apoptosis (**Figure 6D**).

In conclusion, in the spleen of *Gata1^{low}* mice significant levels of megakaryocytes emperipolesis with neutrophils (and electron-hollow para-apoptosis) are observed before significant numbers of activated fibrocytes and peripolesis of these cells with megakaryocytes (and electron-dense para-apoptosis) are detectable, suggesting that the first interaction may be responsible for inducing the second one.

Megakaryocytes represent the spleen cell population expressing the greatest levels of TGF-β

Although TGF-β is produced by almost all cell types [22], immuno-histochemistry studies determined megakaryocytes as the only cells of the spleen from *Gata1^{low}* mice and PMF patients expressing abnormally high levels of TGF-β (**Figure 1C** and [15]). To confirm this observation, immuno-TEM studies with TGF-β antibodies, a technology that allows a better appreciation of the cellular distribution of a protein, were performed (**Figures 8** and **9**).

In addition to megakaryocytes, TGF-β-gold particles were detected in the cytoplasm of neutrophils (**Figure 8**) and activated fibrocytes (**Figure 9**). The numbers of TGF-β-gold particles detected in the cytoplasm of neutrophils increased with age reaching a peak at 6-10-months (82±14 gold particles/cell). However, they remained similar to those observed in neutrophils from wild-type littermates (93±8 gold/paticle/cell by 17-months) (**Figure 9C** and data not shown). At 3-months, few TGF-β-gold particles were detected in the protrusion of the only two activated fibrocytes recognized in spleen sections (one of which presented in **Figure 9A**).

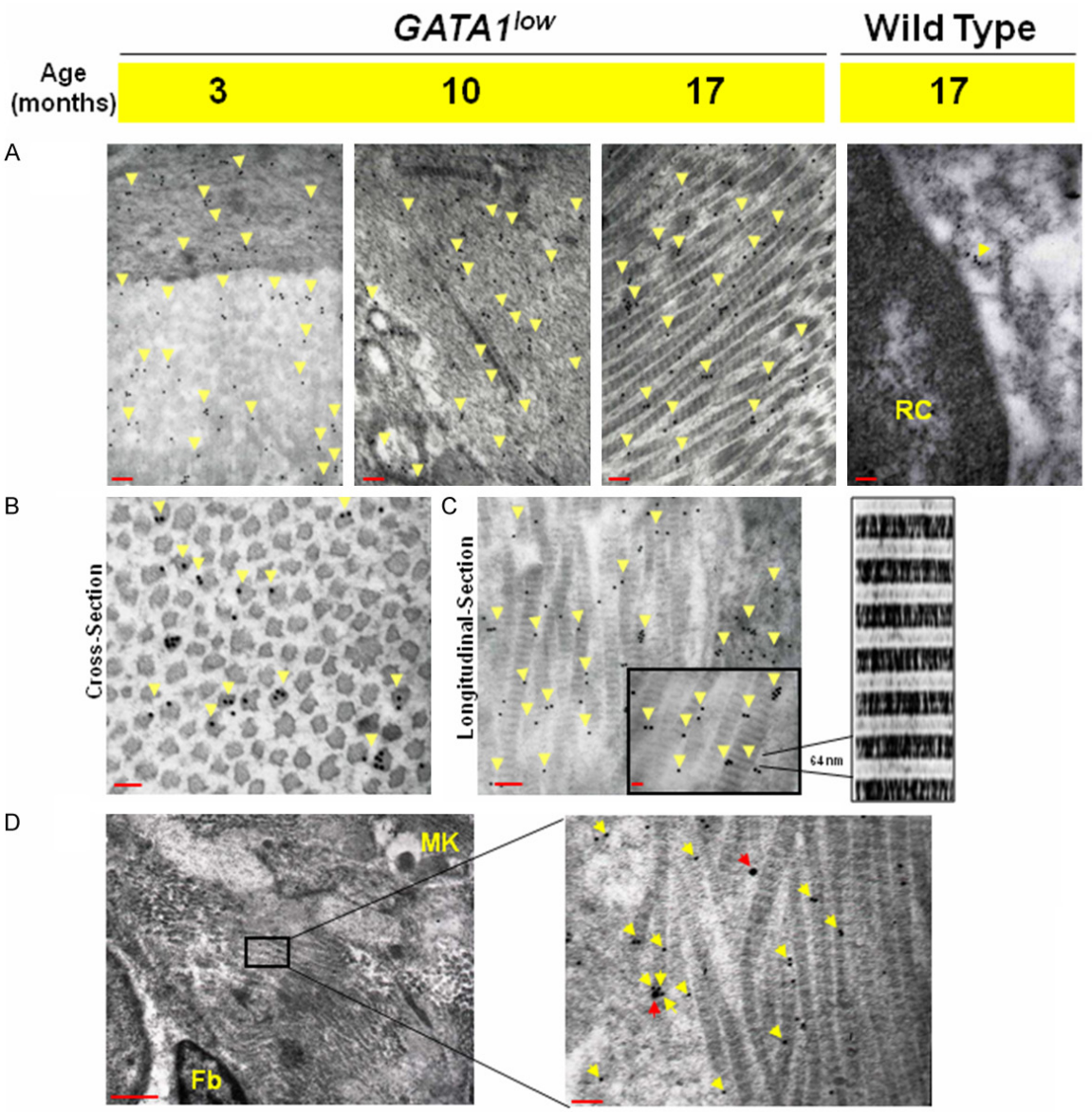

Figure 12. *The spleen from Gata1^{low} mice contains "TGF-β-collagen hot spots".* A. Immuno-TEM for TGF-β of extracellular areas of spleen sections from progressively older *Gata1^{low}* mice. Mature collagen polymers are recognized for their distinctive sequence of light and heavy electron-dense bands, with a 64 nm periodicity. Both the frequency of TGF-β-gold particles and that of mature collagen fibres increases with disease progression (see also **Figure 6**). The spleen from old wild-type littermates contain rare collagen fibres (not shown) and few TGF-β-gold particles, an example of which is indicated by the arrowheads near a red cell (RC), presented as size reference. Magnifications correspond to 4,400x. Scale bars indicate 2 mm length. B, C. Cross- and longitudinal-sections of representative collagen fibres from spleen of 17-months old *Gata1^{low}* mouse immuno-stained for TGF-β. The cross-section shows the selective association of the TGF-β-gold particles, recognized by their shape and size, with the collagen fibres while the longitudinal-section shows that these particles are specifically associated with the heavy electron-dense band of the polymer repeats that corresponds to the non-overlapping region of the fibre twist. Magnifications 50,000x. Scale bars indicate 100 nm. D. Double immuno-gold staining identifying co-localization of TGF-β (yellow arrows), myeloperoxidase (red arrows) and collagen fibres (by morphology) within the cytoplasm of a para-apoptotic megakaryocyte localized in the proximity of a fibrocyte. The area in the rectangle is analyzed at higher magnification on the right to show the relative localization of TGF-β (10 nm, yellow arrowheads)- and myeloperoxidase (20 nm, red arrowheads)-gold particles. Magnifications 4,400x and 30,000x in the panel on the left and in its detail on the right. Scale bars indicate 2 mm on the right and 0.2 mm on the left. Legend: Fb = activated fibrocytes; MK = megakaryocyte; red arrows = myeloperoxidase; yellow arrow = TGF-β.

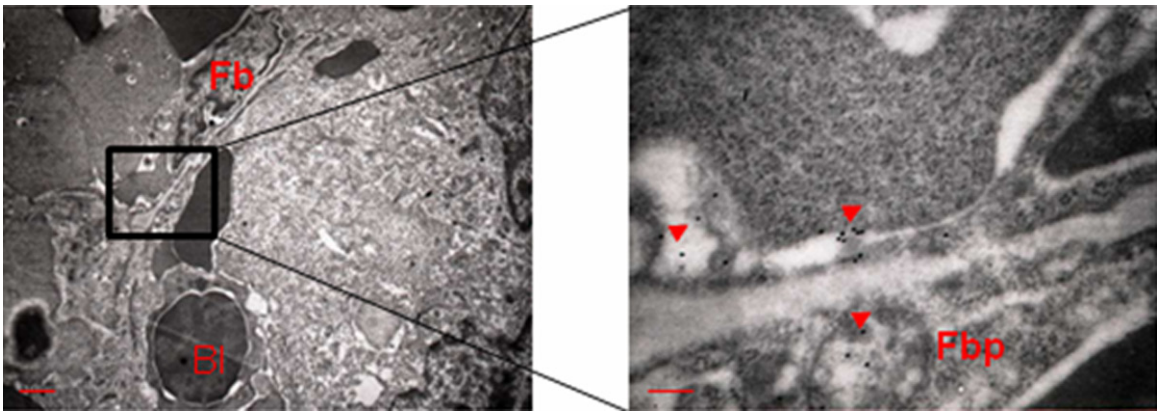

Figure 13. *Immuno-TEM for collagen of a representative activated fibrocytes from spleen the of a 10-month old Gata1^{low} mouse.* The rectangle on the left panel indicates the area of shown at greater magnification on the right. Legend: Bl = blasts; Fb = activated fibrocyte; Fbp = fibrocyte protusion; arrowheads = clusters of collagen-gold particles. Magnifications 4,400x and 30,000x in the left and right panel. Scale bars indicate 2 mm and 0.2 mm in the left panel and right panel.

At 6-10-months the protrusions of activated fibrocytes contained numerous TGF-β-gold particles (61±14 gold particle/14 μm^2) but these numbers decreased (36±9 gold particles/14 μm^2) by 17-months. It is impossible to compare the number of TGF-β-gold particles present in fibrocytes from *Gata1^{low}* and wild-type mice due the limited numbers of cells (only 2) detected in spleen from wild-type mice.

Megakaryocytes were by far the cells that contained the greatest numbers of TGF-β-gold particles (~68-178 gold particles/14 mm^2 of cytoplasm) (**Figure 9B** and **9C**). TGF-β-gold particles were detected both in viable and in para-apoptotic megakaryocytes. By 3-months, the number of TGF-β-gold particles detected in viable megakaryocytes was similar to that present in megakaryocytes from 17-months old wild-type littermates but increased by 3-fold at 6-10-months to return to baseline levels at 17-months. In para-apoptotic megakaryocytes, the number of TGF-β-gold particles increased by 3-fold at 6-10-months and remained high at 17-months. The two para-apoptotic megakaryocytes detected in the spleen of 17-months of wild-type mice expressed one 0 and the other one 117 TGF-β-gold particles/14 mm^2.

These results indicate that in the spleen of *Gata1^{low}* mice TGF-β is also expressed by neutrophils and activated fibrocytes but that the cells in which this growth factor is expressed at the greatest levels are the megakaryocytes and, by 17-months, megakaryocytes undergoing para-apoptosis.

Accumulation of TGF-β associated with collagen fibres in the spleen of Gata1^{low} mice with disease progression

Immuno-histochemistry of consecutive sections of the spleen from *Gata1^{low}* mice reacted progressively more strongly with staining specific for reticulininc fibres (Gomory-Silver, **Figure 10A**) and for those with complex tertiary structures (Mallory Trichromic, **Figure 10B**, and Weighert Van Gieson, **Figure 10C**), confirming that in myelofibrosis progressive accumulation of proteins of the extracellar matrix is associated with increased complexity of their tertiary structure. These results were confirmed by immuno-TEM observations with collagen-specific antibodies.

By immuno-TEM, few collagen-gold particles (11±1/14 μm^2) were detected in the extracellular region of the spleen already at 3-months of age. Their frequencies increased by 20-fold at 10-17-months (~270-290 gold particles/14 μm^2) (**Figure 11**). In agreement with the immuno-histochemical observations, TEM structures corresponding to mature collagen polymers were not detectable in the extracellular region of spleen from 3-months old *Gata1^{low}* mice (**Figure 12A**). These structures became detectable at 6-10-months and formed large areas of multi-stranded fibres, at times inter-crossing each other, at 17-months (**Figure 12A**). There-

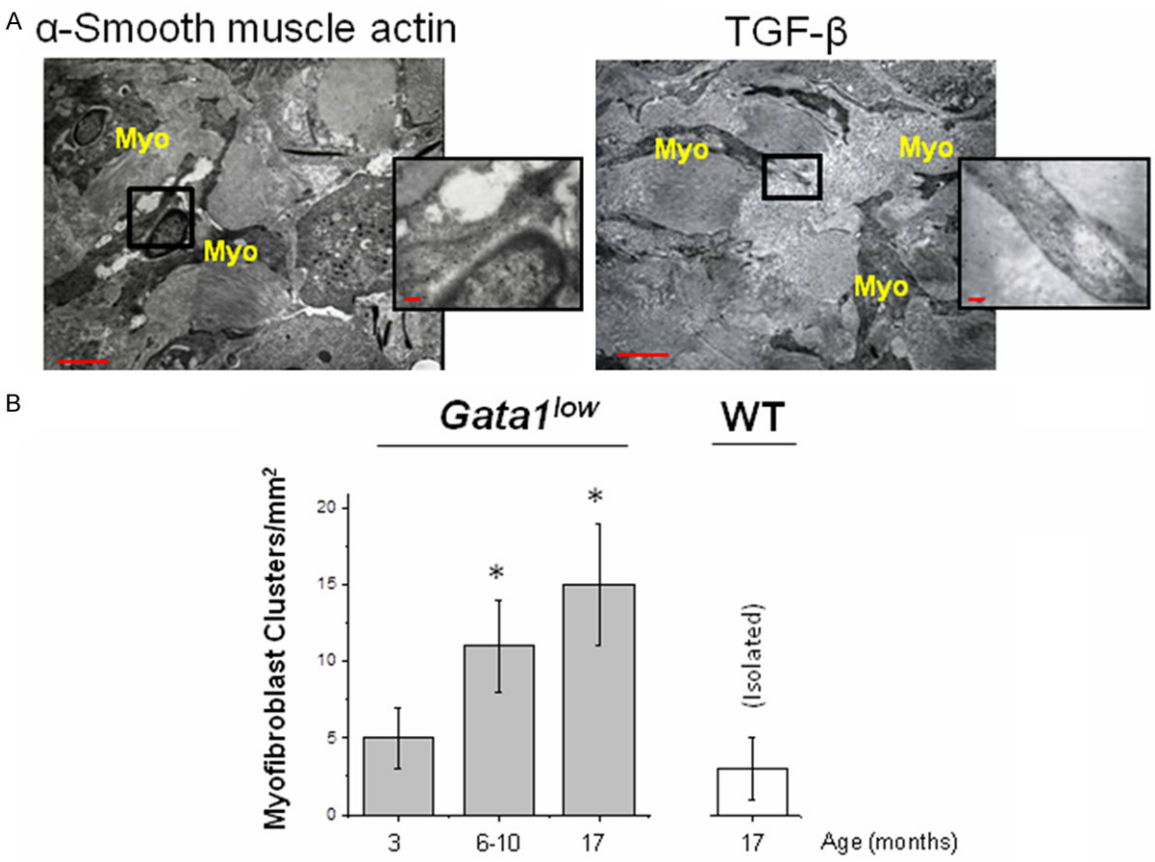

Figure 14. *Increased numbers of myofibroblasts in the spleen of Gata1^{low} mice with disease progression.* A. Immuno-TEM for α-smooth muscle actin and TGF-β of the spleen from a 17-months old *Gata1^{low}* mouse showing representative myofibroblasts (Myo) recognized for their morphology and for their strong reactivity with the α-smooth muscle actin antibody of areas of their cytoplasm organized in fibril-like structures similar to those necessary to exert contracting activity [45]. Myofibroblasts are organized in clusters nested in extracellular areas containing collagen fibres and resembling the cytoplasmic ghosts of megakaryocytes that had died by electron-dense para-apoptosis. These cells also reacted strongly with the TGF-β-antibody. Legend: Myo = myofibroblasts. Magnifications 4,400x in the panels and 30,000x in the inserts. Scale bars indicate 2 mm in the panels and 0.2 mm in the inserts. B. Quantification of the frequency of myofibroblasts clusters from the spleen of *Gata1^{low}* mice during disease progression (3-, 6-10- and 17-months). Values observed with 17-months old wild-type mice are reported for comparison. Results are presented as Mean (±SD) of observations performed with at least three mice per experimental group. * indicates values statistically significant ($p<0.05$ by Anova) with respect to those observed in wild-type mice.

fore, although collagen is detectable in the extracellular matrix of *Gata1^{low}* spleen already at 3-months, it does not form mature complexes before 6-10-months. These mature collagen fibres were not detectable in the proximity of activated fibrocytes (**Figures 3C**, **3D** and **13**) but rather in areas surrounding megakaryocytes (**Figure 4C**).

Increases in the complexity of the collagen structures occurring with disease progression were associated with accumulation of TGF-β-gold particles in the extracellular areas. The extracellular space of the spleen from young *Gata1^{low}* mice contained some (16±1/14 μm) TGF-β-related-gold particles which were not associated with structures recognizable as collagen by TEM (**Figures 12A** and **11**). During disease progression, the frequency of TGF-β-gold particles in these regions increased 2-3-fold (46±13/14 μm and 69±9/14 μm at 6-10- and 17-months, respectively). In the spleen from 17-months old animals, TGF-β-gold particles were only detected in regions of the extracellular matrix containing structures recognizable as mature collagen polymers (**Figure 12A**). Observations at greater magnifications of cross (**Figure 12B**) and longitudinal (**Figure 12C**) sections of collagen polymers indicated that TGF-β-gold staining was specifically associated

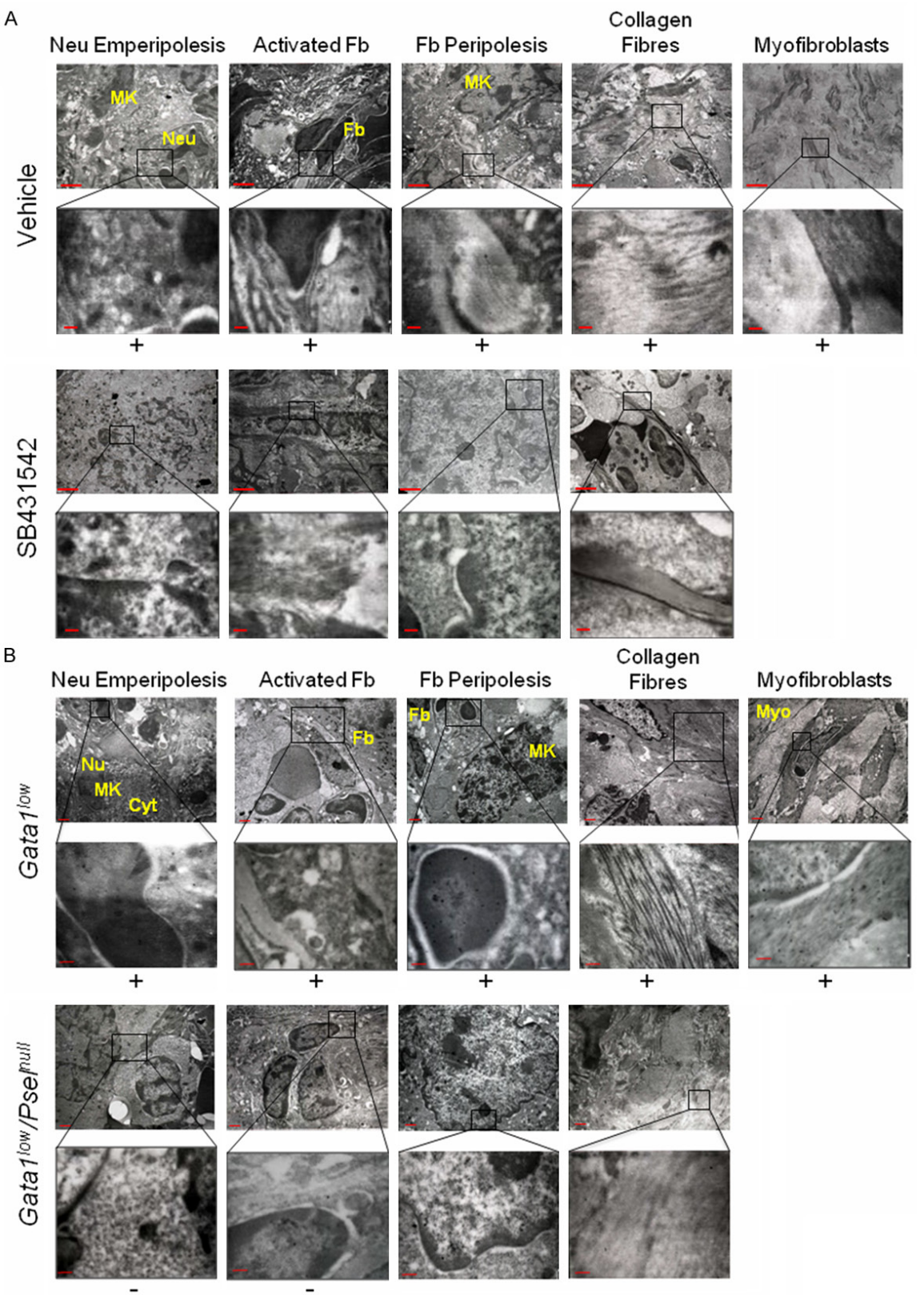

Figure 15. *Both treatment with the TGF-β receptor 1 kinase inhibitor SB431542 and genetic ablation of the P-selectin gene rescued the myelofibrotic phenotype of spleen from Gata1^{low} mice.* (A) Immuno-TEM for TGF-β of spleens from representative *Gata1^{low}* mice treated with vehicle (top panels) or with SB431542 showing that treatment with

the inhibitor reduced to barely detectable levels (indicated with as -) the numbers of megakaryocytes engaged in neutrophil emperipolesis (panels in the first vertical raw), fibrocyte activation (panels in the second vertical raw), engagement of megakaryocytes with fibroblast peripolesis (panels in the third vertical raw), presence of collagen fibres in extracelluar areas (panels in the fourth vertical raw) and of myofibroblasts (panels in the fifth vertical raw). These events were readily recognized in spleen from *Gata1^{low}* littermates treated with vehicles (indicated as +). Rectangles in the first and third horizontal raw indicate areas presented at greater magnification in panels in the second and fourth ones to show the TGF-β-gold particles. Results are representative of those obtained in three animals per experimental group. (B) Immuno-TEM for TGF-β of spleens from representative 17-months old *Gata1^{low}* littermates carrying either the *P-selectin^{null}* (*Psel^{null}*) or *P-selectin wild-type* (*Psel^{wt}*) gene. Similar results were observed with mice of 3- and 6-10-months of age. Results are presented in the same order and are similar to those presented in (A). In this case, they are representative of those observed with a total of 18 *Gata1^{low}* mice (9 *Psel^{null}* and 9 *Psel^{wt}*, three per each age group). The results are equivalent to those described in (A). Legend: Cyt = cytoplasm; Fb = fibrocyte; MK = megakaryocyte; Myo = myofibroblasts; Neu = neutrophil. Magnifications 4,400x and 30,000x in the top and bottom panels, respectively. Scale bars indicate 2 mm in the panels and 0.2 μm in the inserts.

within the dark electron-dense areas corresponding to the non-overlapping areas of the collagen polymer twist, suggesting that TGF-β may have been cross-linked to a specific domain of the protein. By contrast, rare clusters of 1-3 TGF-β-gold particles were detected in the intracellular space of the spleen from old wild-type animals (**Figure 12B**).

Particularly revealing were images obtained by double immune-TEM with TGF-β and myeloperoxidase antibodies of spleen sections from 17-months old *Gata1^{low}* mice such as those presented in **Figure 12D**. The cytoplasm of this electron-dense para-apoptotic megakaryocyte in peripolesis with an activated fibrocyte contained numerous collagen fibres hosting both TGF-β- and myeloperoxidase-gold particles in close association. This image suggests that the megakaryocyte was also engaged in peripolesis with neutrophils that had released myeloperoxidase in its cytoplasm (**Figure 12D**). In addition, the proximity (in some cases <10 nm) of TGF-β- and myeloperoxidase-gold particles suggests that the enzyme was sufficiently close to TGF-β to be able, by exerting its proteolytic functions, to activate its functions.

These results indicate that polymerization of collagen into fibres in the spleen of *Gata1^{low}* mice is a late event in disease progression and that these fibres may provide a scaffolding that increases the bioavailability of TGF-β in the microenvironment to levels ~1000-fold greater than normal.

TGF-β in association with collagen fibres is permissive for myelofibroblast differentiation

Studies in would healing and renal fibrosis indicate that high levels of TGF-β induce the transition of various cell types to myelofibroblasts [46-49]. In agreement with this knowledge, immuno-TEM observations with antibodies specific for a-smooth muscle actin readily identified clusters of 2-5 myofibroblasts in the spleen of *Gata1^{low}* mice (**Figure 14**). These cells reacted strongly with TGF-β antibodies and were nested in areas of the extracellular matrix with features resembling cytoplasmic ghosts of electron-dense para-apoptotic megakaryocytes (compare the background of **Figure 14** with that of the megakaryocytes in the last panels of **Figure 4C** and in **Figure 12D**). The frequency of these clusters significantly increased by 3-fold with disease progression (from ~5 to ~15/mm^2). Calculating that on average each cluster contained ~3 myofibroblasts, the spleen of a 17-months old *Gata1^{low}* mice contains ~45 myofibroblasts/mm^2. By contrast, ~3 isolated myofibroblasts/mm^2 were detected in spleen from 17-months old wild-type littermates.

These results suggest that in spleen of *Gata1^{low}* mice TGF-β bound to collagen fibres is permissive for myofibroblast differentiation and therefore it is biologically active (i.e., TGF-β-loaded collagen fibres may represents “hot spots” for cell differentiation.

Loss of either TGF-β or P-selectin function prevents the formation of TGF-β-collagen hot spots in the spleen of Gata1^{low} mice

To confirm that TGF-β-collagen hot spots are responsible for fibrosis and that their formation is dependent both on TGF-β itself, which induce fibrocyte activation, and P-selectin, which mediates the interaction of megakaryocyte with neutrophils and activated fibrocytes, loss-of-function studies were performed. Loss-of-function TGF-β were induced by treatment with the

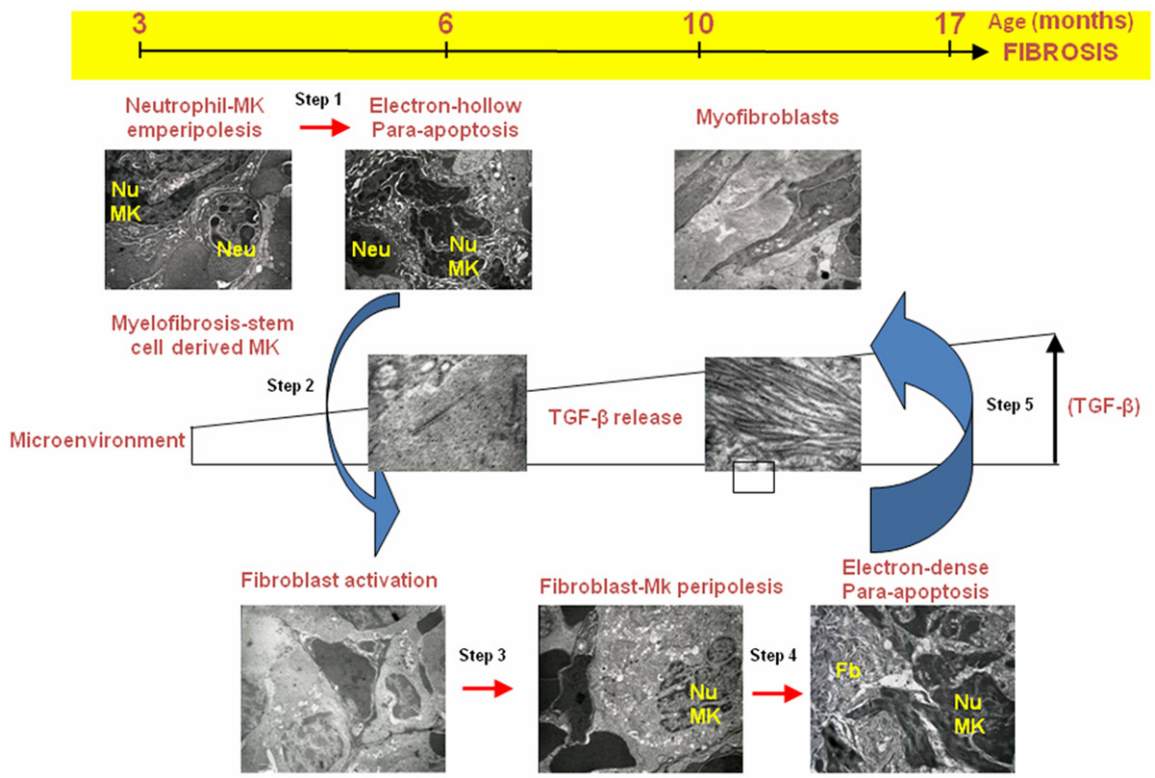

Figure 16. *A model depicting the sequence of pathological interactions between megakaryocytes and immuno cells (neutrophils and activated fibrocytes) leading to fibrosis and myofibroblast differentiation revealed by snap-shot immuno-TEM observations of the spleen from Gata1^{low} mice.* Step 1: 3-months. P-selectin-dependent pathological emperipolesis with neutrophil induces megakaryocytes into electron-hollow para-apoptosis releasing soluble possibly activated TGF-β in the microenvironment ([13] and **Figures 6B**, **12A**). Step 2-3: 6-10-months. Soluble TGF-β induce a resident cell population of the spleen into activated fibrocytes (**Figure 3**). Activated fibrocytes engage into a process of pathological peripolesis with megakaryocytes (**Figures 4**, **6**). Also this process may be P-selectin-dependent. Step 4: 6-10-months. Peripolesis with activated fibrocytes induces megakaryocytes into electron-dense para-apoptosis (**Figures 4**, **6**) which results in the formation of "TGF-β-collagen hot spots" in which the bioavailability of the growth factor reaches levels ~1000-fold greater than normal (**Figure 12**). Step 5: 10-17-months. "TGF-β-collagen hot spots" are permissive for myofibroblast differentiation (**Figure 14**). Legend: Fb = fibrocytes; MK = megakaryocyte; Neu = neutrophil; Nu = nucleus.

TGF-β receptor 1 kinase inhibitor SB431542 while that of P-selectin were obtained by genetic ablation.

The effects of treatment with SB431542 on the cellular composition of the spleen from *Gata1^{low}* mice are presented in **Figure 15A**. Age and sex matched littermates treated with vehicle were analyzed as control. The spleen from SB431542-treated mice did not contain detectable numbers of megakaryocytes engaged in neutrophil emperipolesis or with nuclear features of para-apoptotic cells. In addition, it did not contain fibrocytes in an active state or engaged in peripolesis with megakaryocytes. Furthermore, the extracellular space of the spleen did not contain collagen fibres or myofibroblasts. All these immuno-TEM features were instead detectable in spleens from vehicle-treated mice at levels comparable to those observed in spleen from untreated littermates (compare the top panels of **Figure 15A** and those presented in **Figures 3B**, **3D**, **8C**, **11B** and **12B**).

The effects of genetic ablation of *P-selectin* (*Psel^{null}*) are presented in **Figure 15B**. Also the spleen from *Gata1^{low}/Psel^{null}* mice did not contain megakaryocytes with para-apoptotic features or undergoing neutrophil peripolesis. These sections contained few fibrocytes but the cells did not have an activated morphology and were not engaged in peripolesis with megakaryocytes. Both the megakaryocytes and the

extracellular space in the spleen from double mutant mice contained levels of TGF-β-gold particles within normal ranges. Furthermore, neither collagen fibres nor myofibroblast clusters were detected in these sections. All these structures were instead frequently detected in the spleen of *Gata1^{low}* littermates wild-type at the *P-selectin* locus.

Discussion

The great magnifications achievable by immune-TEM technology allowed determining that the bioavailability of TGF-β in the spleen of *Gata1^{low}* mice reaches levels ~1,000-fold greater than normal. These levels are achieved because TGF-β became physically associated, possibly by enzymatic cross-linking, with specific regions of the collagen fibres, the D bands, which also mediate binding of collagen to decorin, a protein responsible for binding collagen to other elements of the extracellular matrix [43]. These results identify collagen as a novel element of the extracellular matrix that, in addition to fibrillin-1 [27], may regulate bioavailability of TGF-β in the microenvironment. We suggest that the bioavailability of TGF-β regulated by collagen plays in chronic inflammation the same morphogenetic role played by fibrillin-1 in bone development [25].

Snap-shot immuno-TEM observations of the spleen from *Gata1^{low}* mice during disease progression indicated that in myelofibrosis TGF-β bioavailability is increased by a complex mechanism involving pathological interactions between multiple cell types (see **Figure 16**). Since in *Gata1^{low}* mice the disease progresses in a timely fashion and hematopoiesis is limited to the spleen, a large soft organ amenable to extensive microscopic observations, it was possible, by comparing snap-shots obtained at different ages, to identify the sequence of events that increased TGF-β bioavailability in this mouse model.

At 3-months, the spleen from *Gata1^{low}* mice contained numerous electron-hollow para-apoptotic magakaryoctes engaged in pathological emperipolesis with neutrophils. These cells contained great levels of TGF-β and were probably the source of TGF-β found in the extracellular space at this age.

At 6-10 months, the spleen from *Gata1^{low}* mice contained many activated fibrocytes, a cell population that has been implicated in disease progression in animal models of fibrosis of kidney [50], lung [51, 52] and heart [53] failure. The cell population which becomes activated fibrocytes in the spleen of *Gata1^{low}* mice has not been positively identified as yet. In fact, the frequency of cells with the phenotype CD45^{neg}/PDGF-R^{pos} (activated fibrocyte of endothelial origin) or CD45^{pos}/PDGF-R^{pos}/F4/80^{pos} (activated fibrocytes of macrophagic origin) [47, 54] in these spleen is normal [55]. In addition, activated fibrocytes were never observed in proximity of vessels (identified on the basis of CD31-gold staining, data not shown) suggesting that they are unlikely to derive from pericytes, a population responsible for fibrosis in obstructive kidney fibrosis [56-59]. The identification of the cell population that undergoes mesenchymal transition in the spleen of *Gata1^{low}* mice will be the subject of a separate study.

Loss of TGF-β function by treatment with a TGF-β receptor 1 kinase inhibitor prevented induction of activated fibrocytes in the spleen of Gata1^{low} mice, providing evidence that this growth factor is indeed responsible for the mesenchymal transition that had generated them. The observations that pathological emperipolesis between megakaryocyte and neutrophils is detectable at high frequency by 3-months, i.e. before significant numbers of activated fibrocytes were detected, and that TGF-β and activated fibrocytes were both undetectable in the spleen of *Gata1^{low}* mice lacking *P-selectin*, the receptor which mediates the interaction between megakaryocytes and neutrophils [10], indicates that electron-hollow megakaryocytes are probably the source of TGF-β that induced the formation of activated fibrocytes.

With disease progression, great numbers of activated fibrocytes were observed engaged in a pathological interaction with megakaryocytes defined by us peripolesis. During this interaction, the protrusions of the activated fibrocyte embraced the megakaryocyte infiltrating its cytoplasm. Based on snap-shot immune-TEM observations, we identify a series of megakaryocyte images that probably correspond to cells at progressive stages of peripolesis. The comparison of these images indicates that the interaction may involve progressive reductions in the numbers of collagen-gold particles in the

protrusions and parallel increases in those in the megakaryocyte cytoplasm. By extrapolating these static observations to a dynamic state, we propose that fibrocytes actively transfer collagen, and possibly other material, to the megakaryocyte cytoplasm. Therefore peripolesis is not a form of phagocytosis but rather a novel cellular interaction involving active passage of material from one cell to another. Whether pathological peripolesis between activated fibrocytes and megakaryocytes is restricted to myelofibrosis or occurs also in other pathologies, including some forms of cancer, remains to be established.

In spite of the great levels of collagen expressed by activated fibrocytes, the extracellular space in their immediate proximity contained few collagen-gold particles and no collagen fibres. These observations indicated that it is unlikely that in myelofibrosis collagen fibres are polymerized by LOX2 released by megakaryocytes in the extracellular space. Instead, starting from 6-10-months of age, collagen fibres were frequently detected in close proximity or even within electron-dense para-apoptotic megakaryocytes. Snap-shot observations of megakaryocytes in various stages of interaction with activated fibrocytes indicated that in the early stages of the process their cytoplasm contained only collagen-gold particles and that polymerized collagen appeared at later stages. Therefore, by contrast with current believe [41], in the spleen of *Gata1^{low}* mice LOX2 may exert its catalytic function and catalyze collagen polymerization also inside the megakaryocyte cytoplasm. Ultrastructure features indicative for accumulation of collagen fibres inside the cytoplasm were detected at high frequency also in megakaryocytes from the spleen of PMF patients suggesting that a mechanism(s) similar to that outlined here for *Gata1^{low}* mice is responsible for fibrosis in the patients as well. This consideration indicates that strategies to treat PMF with LOX2 inhibitors currently under consideration [60] should include methods to increase their intracellular delivery.

At late stages of peripolesis, megakaryocytes acquired the morphology of para-apoptotic cells with electron-dense cytoplasm suggesting that their interaction with activated fibrocytes resulted to death. This form of para-apoptosis is novel and further studies are required to assess if activated fibrocytes induce para-apoptosis only of megakaryocytes or may use a similar mechanism to induce death of other cell types. Electron-dense para-apoptosis lead to the formation of cytoplasmic ghosts filled with collagen fibres loaded with TGF-β and surrounding naked nuclei. Extensive TEM observations allowed assessing that these ghosts are the main source of fibrosis in the spleen of *Gata1^{low}* mice.

Circumstantial evidences that TGF-β bound to collagen fibres is biologically active were provided by double immuno-TEM observations which identified that TGF-β- and myeloperoxidase-gold particles were closely associated on the collagen fibres and that these areas also contained myofibroblasts, a cell population which is specifically induced by high TGF-β concentrations. Therefore, by contrast with obstructive [56] and diabetic interstitial [61] kidney fibrosis, in *Gata1^{low}* mice myofibroblast differentiation is the consequence and not the cause of collagen deposition.

It is currently debated whether a “single” drug may be effective for treating fibrosis in fatal failure of different organs. Our results indicating that myelofibrosis is induced by mesenchymal transitions of a cell population different from that active in other organs suggest that this may not be the case. Further support for this hypothesis comes from the consideration that *Gata1^{low}* mice were treated by an inhibitor targeting the TGF-β receptor 1 kinase ALK5 ([55] and this manuscript) while animal models of kidney fibrosis were rescued by treatment with inhibitors of the TGF-β receptor 2 kinase ALK3 [62]. In addition, both in models of cardiac fibrosis [53] and of chronic renal injury [63] endothelial cells to mesenchymal transition was inhibited by recombinant human BMP-7, a protein that inhibits the canonical SMAD-dependent TGF-β signaling. By contrast, BMP-7 is expressed at levels 10-fold greater than normal by marrow a spleen from both PMF patients [35] and *Gata1^{low}* mice [15] that are characterized by abnormalities predictive of activation of non-canonical ERK/MAPK-dependent rather than canonical TGF-β signaling. We suggest that TGF-β receptor 1 kinase inhibitors targeting ALK5, such as galunisertib that target this enzyme with an ID_{50} 2-fold higher than SB431542 (ID_{50} = 48 vs 94 nM) [64, 65], are best suited for treatment of PMF.

In conclusion, our snap-shot observations of the morphological changes occurring in spleen from *Gata1^{low}* mice with disease progression suggest the following pathobiological pathway (**Figure 16**). In young mice, abnormal localization of P-selectin on the DMS of *Gata1^{low}* megakaryocytes induces pathological neutrophil emperipolesis that release the neutrophil proteolytic enzymes into the megakaryocyte cytoplasm, inducing its para-apoptotic death and release soluble TGF-β, in the microenvironment. Soluble TGF-β induces the transition of a resident cell population of the spleen, still to be identified, into activated fibrocytes. Through their long protrusions, activated fibrocytes engage into a peripolesis process with megakaryocytes releasing collagen in their cytoplasm. This interaction may also be P-selectin dependent. Once infiltrated by fibrocyte protrusions, megakaryocytes became engulfed with collagen which is polymerized by the high levels of LOX2 present in these cells. During this polymerization process, an enzyme, either LTBP, decorin or a protein still to be identified, cross-links TGF-β, and possibly proteases released by emperipolesized neutrophils, to collagen. Collagen-embedded megakaryocyte die of electron-dense para-apoptosis releasing TGF-β-cross-linked to collagen fibres in the microenvironment and increasing its bioavailability. These areas of TGF-β-collagen represent "hot spots" permissive for myofibroblast differentiation. Whether myofibroblasts play any role in the manifestation of myelofibrosis in Gata1^{low} mice is unclear.

Acknowledgements

This study was supported the National Cancer Institute (P01-CA108671) (ARM), Associazione Italiana Ricerca sul Cancro (AIRC 10413) (ARM) and Programma FIRB 2010 (RBAP10447J_005) (RAR). Dr. Gianni Barosi is gratefully acknowledged for providing spleens from non-diseased donors and PMF patients.

Disclosure of conflict of interest

None.

Address correspondence to: Dr. Anna Rita Migliaccio, Tisch Cancer Institute, Ichan School of Medicine at Mount Sinai, One Gustave L Levy Place, Box #1079, New York, NY 10029, USA. Tel: 212-241-6974; Fax: 212-876-5276; E-mail: annarita.migliaccio@mssm.edu

References

[1] Tefferi A. Myelofibrosis with myeloid metaplasia. N Engl J Med 2000; 342: 1255-1265.
[2] Skoda RC, Duek A, Grisouard J. Pathogenesis of myeloproliferative neoplasms. Exp Hematol 2015; 43: 599-608.
[3] Tefferi A, Thiele J, Vannucchi AM, Barbui T. An overview on CALR and CSF3R mutations and a proposal for revision of WHO diagnostic criteria for myeloproliferative neoplasms. Leukemia 2014; 28: 1407-1413.
[4] Lacout C, Pisani DF, Tulliez M, Gachelin FM, Vainchenker W, Villeval JL. JAK2V617F expression in murine hematopoietic cells leads to MPD mimicking human PV with secondary myelofibrosis. Blood 2006; 108: 1652-1660.
[5] Zucker-Francklin D. Ultrastructural studies of hematopoietic elements in relation to the myelofibrosis-osteosclerosis syndrome, megakaryocytes and platelets (MMM or MOS). In: Burkhardt R CC, Lennert K, Adler SS, Pincus T, Till JE (eds) Workshop on Muelofibrosis-osteosclerosis syndrome. Dahlem, West Germany, 1975, pp. 127-1435.
[6] Martyré MC, Romquin N, Le Bousse-Kerdiles MC, Chevillard S, Benyahia B, Dupriez B, Demory JL, Bauters F. Transforming growth factor-beta and megakaryocytes in the pathogenesis of idiopathic myelofibrosis. Br J Haematol 1994; 88: 9-16.
[7] Schmitt A, Jouault H, Guichard J, Wendling F, Drouin A, Cramer EM. Pathologic interaction between megakaryocytes and polymorphonuclear leukocytes in myelofibrosis. Blood 2000; 96: 1342-1347.
[8] Vannucchi AM, Pancrazzi A, Guglielmelli P, Di Lollo S, Bogani C, Baroni G, Bianchi L, Migliaccio AM, Bosi A, Paoletti F. Abnormalities of GATA-1 in megakaryocytes from patients with idiopathic myelofibrosis. Am J Pathol 2005; 167: 849-858.
[9] Etulain J, Martinod K, Wong SL, Cifuni SM, Schattner M, Wagner DD. P-selectin promotes neutrophil extracellular trap formation in mice. Blood 2015; 126: 242-246.
[10] Mayadas TN, Johnson RC, Rayburn H, Hynes RO, Wagner DD. Leukocyte rolling and extravasation are severely compromised in P selectin-deficient mice. Cell 1993; 74: 541-554.
[11] Thiele J, Lorenzen J, Manich B, Kvasnicka HM, Zirbes TK, Fischer R. Apoptosis (programmed cell death) in idiopathic (primary) osteo-/myelofibrosis: naked nuclei in megakaryopoiesis reveal features of para-apoptosis. Acta Haematol 1997; 97: 137-143.

[12] Speradio S, de Belle I, Bredesen DE. An alternative, non-apoptotic form of programmed cell death. Proc Natl Acad Sci U S A 2009; 97: 14376-14381.
[13] Centurione L, Di Baldassarre A, Zingariello M, Bosco D, Gatta V, Rana RA, Langella V, Di Virgilio A, Vannucchi AM, Migliaccio AR. Increased and pathologic emperipolesis of neutrophils within megakaryocytes associated with marrow fibrosis in GATA-1^{low} mice. Blood 2004; 104: 3573-3580.
[14] Chagraoui H, Komura E, Tulliez M, Giraudier S, Vainchenker W, Wendling F. Prominent role of TGF-beta 1 in thrombopoietin-induced myelofibrosis in mice. Blood 2002; 100: 3495-3503.
[15] Zingariello M, Martelli F, Ciaffoni F, Masiello F, Ghinassi B, D'Amore E, Massa M, Barosi G, Sancillo L, Li X, Goldberg JD, Rana RA, Migliacco AR. Characterization of the TGF-beta1 signaling abnormalities in the Gata1^{low} mouse model of myelofibrosis. Blood 2013; 121: 3345-3363.
[16] Bobik R, Dabrowski Z. Emperipolesis of marrow cells within megakaryocytes in the bone marrow of sublethally irradiated mice. Ann Hematol 1995; 70: 91-95.
[17] Lee KP. Emperipolesis of hematopoietic cells within megakaryocytes in the bone marrow of the rat. Vet Pathol 1989; 26: 473-478.
[18] McGarry MP, Reddington M, Jackson CW, Zhen L, Novak EK, Swank RT. Increased incidence and analysis of emperipolesis in megakaryocytes of the mouse mutant gunmetal. Exp Mol Path 1999; 66: 191-200.
[19] Campanelli R, Rosti V, Villani L, Castagno M, Moretti E, Bonetti E, Bergamaschi G, Balduini A, Barosi G, Massa M. Evaluation of the bioactive and total transforming growth factor β1 levels in primary myelofibrosis. Cytokine 2011; 53: 100-106.
[20] Tefferi A, Vaidya R, Caramazza D, Finke C, Lasho T, Pardanani A. Circulating interleukin (IL)-8, IL-2R, IL-12, and IL-15 levels are independently prognostic in primary myelofibrosis: a comprehensive cytokine profiling study. J Clin Oncol 2011; 29: 1356-1363.
[21] Fleischman AG, Aichberger KJ, Luty SB, Bumm TG, Petersen CL, Doratotaj S, Vasudevan KB, LaTocha DH, Yang F, Press RD, Loriaux MM, Pahl HL, Silver RT, Agarwal A, O'Hare T, Druker BJ, Bagby GC, Deininger MW. TNFα facilitates clonal expansion of JAK2V617F positive cells in myeloproliferative neoplasms. Blood 2011; 118: 6392-6398.
[22] Massagué J, Heino J, Laiho M. Mechanisms in TGF-beta action. Ciba Found Symposium 1991; 157: 51-59.
[23] Massagué J. TGFbeta in Cancer. Cell 2008; 134: 215-230.
[24] Akhurst RJ, Hata A. Targeting the TGFβ signalling pathway in disease. Nat Rev Drug Discov 2012; 11: 790-811.
[25] Smaldone S, Ramirez F. Fibrillin microfibrils in bone physiology. Matrix Biol 2015; 130-134.
[26] Gualandris A, Annes JP, Arese M, Noguera I, Jurukovski V, Rifkin DB. The Latent Transforming Growth Factor-β–binding Protein-1 Promotes In Vitro Differentiation of Embryonic Stem Cells into Endothelium. Mol Biol Cell 2000; 11: 4295–4308.
[27] Nunes I, Gleizes PE, Metz CN, Rifkin DB. Latent transforming growth factor-beta binding protein domains involved in activation and transglutaminase-dependent cross-linking of latent transforming growth factor-beta. J Cell Biol 1997; 136: 1151-1163.
[28] Smaldone S, Clayton NP, Del Solar M, Pascual-Gonzales G, Cheng SH, Wentworth BM, Schaffler MB, Ramirez F. Fibrillin-1 Regulates skeletal stem cell differentiation by modulating TGFβ activity within the marrow niche. J Bone Miner Res 2015; 20: 1-12.
[29] Vyas P, Ault K, Jackson CW, Orkin SH, Shivdasani RA. Consequences of GATA-1 deficiency in megakaryocytes and platelets. Blood 1999; 93: 2867-2875.
[30] McDevitt MA, Shivdasani RA, Fujiwara Y, Yang H, Orkin SH. A "knockdown" mutation created by cis-element gene targeting reveals the dependence of erythroid cell maturation on the level of transcription factor GATA-1. Proc Natl Acad Sci U S A 1997; 94: 6781-6785.
[31] Martelli F, Ghinassi B, Panetta B, Alfani E, Gatta V, Pancrazzi A, Bogani C, Vannucchi AM, Paoletti F, Migliaccio G, Migliaccio AR. Variegation of the phenotype induced by the Gata1^{low} mutation in mice of different genetic backgrounds. Blood 2005; 106: 4102-4113.
[32] Vannucchi AM, Bianchi L, Cellai C, Paoletti F, Rana RA, Lorenzini R, Migliaccio G, Migliaccio AR. Development of myelofibrosis in mice genetically impaired for GATA-1 expression (GATA-1^{low} mice). Blood 2002; 100: 1123-1132.
[33] Meyer SC, Keller MD, Chiu S, Koppikar P, Guryanova OA, Rapaport F, Xu K, Manova K, Pankov D, O'Reilly RJ, Kleppe M, McKenney AS, Shih AH, Shank K, Ahn J, Papalexi E, Spitzer B, Socci N, Viale A, Mandon E, Ebel N, Andraos R, Rubert J, Dammassa E, Romanet V, Dölemeyer A, Zender M, Heinlein M, Rampal R, Weinberg RS, Hoffman R, Sellers WR, Hofmann F, Murakami M, Baffert F, Gaul C, Radimerski T, Levine RL. CHZ868, a Type II JAK2 Inhibitor, Reverses Type I JAK Inhibitor Persistence and Demonstrates Efficacy in Myeloproliferative Neoplasms. Cancer Cell 2015; 28: 15-28.
[34] Arranz L, Sánchez-Aguilera A, Martín-Pérez D, Isern J, Langa X, Tzankov A, Lundberg P,

Muntión S, Tzeng YS, Lai DM, Schwaller J, Skoda RC, Méndez-Ferrer S. Neuropathy of haematopoietic stem cell niche is essential for myeloproliferative neoplasms. Nature 2014; 512: 78-81.

[35] Ciaffoni F, Cassella E, Varricchio L, Massa M, Barosi G, Migliaccio AR. Activation of non-canonical TGF-β1 signaling indicates an autoimmune mechanism for bone marrow fibrosis in primary myelofibrosis. Blood Cells Mol Dis 2015; 54: 234-241.

[36] Tefferi A, Thiele J, Orazi A, Kvasnicka HM, Barbui T, Hanson CA, Barosi G, Verstovsek S, Birgegard G, Mesa R, Reilly JT, Gisslinger H, Vannucchi AM, Cervantes F, Finazzi G, Hoffman R, Gilliland DG, Bloomfield CD, Vardiman JW. Proposals and rationale for revision of the World Health Organization diagnostic criteria for polycythemia vera, essential thrombocythemia, and primary myelofibrosis: recommendations from an ad hoc international expert panel. Blood 2007; 110: 1092-1097.

[37] Frenette PS, Denis CV, Weiss L, Jurk K, Subbarao S, Kehrel B, Hartwig JH, Vestweber D, Wagner DD. P-Selectin glycoprotein ligand 1 (PSGL-1) is expressed on platelets and can mediate platelet-endothelial interactions in vivo. J Exp Med 2000; 191: 1413-1422.

[38] Doyle GD, Campbell E. The periodic acid silver methenamin (PASM) staining of renal biopsies. Light and electron microscopy study. Irish J Med Sci 1976; 145: 127-34.

[39] Puchtler H, Isler H. The effect of phosphomoly bdic acid on the stainability of connective tissues by various dyes. J Histochem Cytochem 1958; 6: 265-270.

[40] Pearse AGE. Histochemistry, theoretical and applied. Edited by Boston Little Brown and Co, 2nd edition, 1960, pp. 165-175, 582-583, 816, 820-821.

[41] Brodsky B, Persikov AV. Molecular structure of the collagen triple helix. Adv Protein Chem 2005; 70: 301-339.

[42] Eliades A, Papadantonakis N, Bhupatiraju A, Burridge KA, Johnston-Cox HA, Migliaccio AR, Crispino JD, Lucero HA, Trackman PC, Ravid K. Control of megakaryocyte expansion and bone marrow fibrosis by lysyl oxidase. J Biol Chem 2011; 286: 27630-27638.

[43] Keene DR, Ridgway CC, Iozzo RV. Type VI microfilaments interact with a specific region of banded collagen fibrils in skin. J Histochem Cytochem 1998; 46: 215-220.

[44] Migliaccio AR, Martelli F, Verrucci M, Sanchez M, Valeri M, Migliaccio G, Vannucchi AM, Zingariello M, Di Baldassarre A, Ghinassi B, Rana RA, van Hensbergen Y, Fibbe WE. Gata1 expression driven by the alternative HS2 enhancer in the spleen rescues the hematopoietic failure induced by the hypomorphic *Gata1^{low}* mutation. Blood 2009; 114: 2107-2120.

[45] Wickenhauser C, Schmitz B, Baldus SE, Henze F, Farahmand P, Frimpong S, Thiele J, Fischer R. Selectins (CD62L, CD62P) and megakaryocytic glycoproteins (CD41a, CD42b) mediate megakaryocyte-fibroblast interactions in human bone marrow. Leuk Res 2000; 24: 1013-1021.

[46] Vaughan MB, Howard EW, Tomasek JJ. Transforming growth factor-beta1 promotes the morphological and functional differentiation of the myofibroblast. Exp Cell Res 2000; 257: 180-189.

[47] LeBleu VS, Taduri G, O'Connell J, Teng Y, Cooke VG, Woda C, Sugimoto H, Kalluri R. Origin and function of myofibroblasts in kidney fibrosis. Nat Med 2013; 19: 1047-1053.

[48] Gabbiani G. The myofibroblast in wound healing and fibrocontractive diseases. J Pathol 2003; 200: 500-503.

[49] Meran S, Steadman R. Fibroblasts and myofibroblasts in renal fibrosis. Int J Exp Pathol 2011; 92: 158-167.

[50] Kriz W, Kaissling B, Le Hir M. Epithelial-mesenchymal transition (EMT) in kidney fibrosis: fact or fantasy? J Clin Invest 2011; 121: 468-474.

[51] Hashimoto N, Phan SH, Imaizumi K, Matsuo M, Nakashima H, Kawabe T, Shimokata K, Hasegawa Y. Endothelial-Mesenchymal Transition in Bleomycin-Induced Pulmonary Fibrosis. Am J Respir Cell Mol Biol 2010; 43: 161-172.

[52] Rock JR, Barkauskas CE, Cronce MJ, Xue Y, Harris JR, Liang J, Noble PW, Hogan BL. Multiple stromal populations contribute to pulmonary fibrosis without evidence for epithelial to mesenchymal transition. Proc Natl Acad Sci U S A 2011; 108: 1475-1483.

[53] Zeisberg EM, Tarnavski O, Zeisberg M, Dorfman AL, McMullen JR, Gustafsson E, Chandraker A, Yuan X, Pu WT, Roberts AB, Neilson EG, Sayegh MH, Izumo S, Kalluri R. Endothelial-to-mesenchymal transition contributes to cardiac fibrosis. Nat Med 2007; 13: 952-961.

[54] Kalluri R, Neilson EG. Epithelial-mesenchymal transition and its implications for fibrosis. J Clin Invest 2003; 112: 1776-1784.

[55] Spangrude GJ, Lewandowski D, Martelli F, Marra M, Zingariello M, Sancillo L, Rana AR, Migliaccio AR. P-Selectin Sustains Extramedullary Hematopoiesis in the Gata1low Model of Myelofibrosis. Stem Cells 2016; 34: 67-82.

[56] Lin SL, Kisseleva T, Brenner DA, Duffield JS. Pericytes and perivascular fibroblasts are the primary source of collagen-producing cells in

obstructive fibrosis of the kidney. Am J Pathol 2008; 173: 1617-1627.
[57] Díaz-Flores L, Gutiérrez R, Madrid JF, Varela H, Valladares F, Acosta E, Martín-Vasallo P, Díaz-Flores L Jr. The bone marrow constitutes a reservoir of pericyte progenitors. Histol Histopathol 2009; 24: 909-969.
[58] Zeisberg EM, Potenta SE, Sugimoto H, Zeisberg M, Kalluri R. Fibroblasts in kidney fibrosis emerge via endothelial-to-mesenchymal transition. J Am Soc Nephrol 2008; 19: 2282-2287.
[59] Humphreys BD, Lin SL, Kobayashi A, Hudson TE, Nowlin BT, Bonventre JV, Valerius MT, McMahon AP, Duffield JS. Fate tracing reveals the pericyte and not epithelial origin of myofibroblasts in kidney fibrosis. Am J Pathol 2010; 176: 85-97.
[60] Santos FP, Verstovsek S. What is next beyond janus kinase 2 inhibitors for primary myelofibrosis? Curr Opin Hematol 2013; 20: 123-129.
[61] Li J, Qu X, Bertram JF. Endothelial-myofibroblast transition contributes to the early development of diabetic renal interstitial fibrosis in streptozotocin-induced diabetic mice. Am J Pathol 2009; 175: 1380-1388.
[62] Sugimoto H, LeBleu VS, Bosukonda D, Keck P, Taduri G, Bechtel W, Okada H, Carlson W Jr, Bey P, Rusckowski M, Tampe B, Tampe D, Kanasaki K, Zeisberg M, Kalluri R. Activin-like kinase 3 is important for kidney regeneration and reversal of fibrosis. Nat Med 2012; 19: 1047-1053.
[63] Zeisberg M, Hanai J, Sugimoto H, Mammoto T, Charytan D, Strutz F, Kalluri R. BMP-7 counteracts TGF-beta1-induced epithelial-to-mesenchymal transition and reverses chronic renal injury. Nat Med 2003; 9: 964-968.
[64] Zhou L, McMahon C, Bhagat T, Alencar C, Yu Y, Fazzari M, Sohal D, Heuck C, Gundabolu K, Ng C, Mo Y, Shen W, Wickrema A, Kong G, Friedman E, Sokol L, Mantzaris I, Pellagatti A, Boultwood J, Platanias LC, Steidl U, Yan L, Yingling JM, Lahn MM, List A, Bitzer M, Verma A. Reduced SMAD7 leads to overactivation of TGF-beta signaling in MDS that can be reversed by a specific inhibitor of TGF-beta receptor I kinase. Cancer Res 2011; 71: 955-963.
[65] Serova M, Tijeras-Raballand A, Dos Santos C, Albuquerque M, Paradis V, Neuzillet C, Benhadji KA, Raymond E, Faivre S, de Gramont A. Effects of TGF-beta signalling inhibition with galunisertib (LY2157299) in hepatocellular carcinoma models and in ex vivo whole tumor tissue samples from patients. Oncotarget 2015; 6: 21614-21627.